Lund University

Lund Institute of Technology

Department of Pure and Applied Biochemistry

Universidade da Beira Interior

Chemistry Department

ACOUSTIC "WALL-LESS" TEST TUBES FOR CELL BIOLOGY IN TYPE 2 DIABETES RELATED RESEARCH

Supervised by:

Prof. Staffan Nilsson

Prof. Ana Cristina Cabral

Sandra Lemos, 831208-P188/M2781

Covilhã, 2008/09/04

Acknowledgements

My return to Lund for another year was again full of new experiences, a year filled with very interesting and pleasant surprises, a year that brought me new knowledge both in science and live. I have, thus, many people to be thankful to. My sincere recognition for all those people who, in one way or another, help to get through the past months in the best way possible:

My enormous gratitude to Prof. Staffan Nilsson, my supervisor at Lund University, for the never ending knowledge, support, and friendship.

To Prof. Ana Cristina Cabral, my supervisor at Portugal, my sincere admiration for all the professionalism and my gratefulness for the prompt availability every time it was required.

To Dr. Niklas Gustavsson and Dr. Wietske Lambert, for teaching me everything I know about mass spectrometry, but also for all the support to my project.

To Dr. Cedric Dicko for teaching me all the "tricks" of the fluorescence system.

Prof. Eva Degerman, for the biological background, time and support.

Dr. Thomas Johansen, Dr. Patrik Rorsman, Dr. Sabina Santesson, as coworkers on the published paper, thanks for the great job.

Dr. Johan Nilsson for the flow-through pL dispensers and prompt assistance.

Dr. Lena Eliasson, for the β-cells.

Eva Ohlson, for the adipocytes and the good advices.

To Curt Reimann and Frederik Pontén, for the large assistance in the "Real-Time" experiments.

All my warmth to "Staffans Group", Christian Nilsson, Susana Carvalho, Magnus Jakobsson, Yu Yang, Loy Alkhafadiji. Thanks for everything.

To all my professors at Universidade da Beira interior for my background.

To all my closest friends, Filipa, David, Sérgio, Mariano, Andreia, Susana, Mariela, and Célia for the everyday support and friendship.

To my beloved parents, Duarte and Felisbela, brother Carlos, for all the love and support. To my year old niece, Matilde for the sweet and relaxing times.

To the remaining family and friends, for the love and affection.

To the Department of Pure and Applied Biochemistry, not only for the discussions about Science but also for the nice and relaxing hours, mainly at the weekly "Cake Mafia".

To Lund University and Universidade da Beira Interior.

Finally, the financial support from Novo Scholarship Program, Nova Nordisk, Vetenskapsrådet (VR 621-2007-4275), Crafoordska Stiftelsen, Kungliga Fysiografiska Sällskapet i Lund, Centrala Försöksdjursnämnden, R. W. Johnson Research Institute and Agência Nacional para a Gestão do Programa de Aprendizagem ao Longo da Vida and the European commission are gratefully acknowledged.

Abstract

New insights into biomedicine and related areas require the parallel development of new analytical methods. A technique for chemical analysis based on the use of acoustically levitated droplets, suitable for the study of intra and extracellular reactions at single or few cells level has been developed. Microenvironments suited for specific cell types and cell reactions can be created in levitated droplets to serve as biomimetic systems.

The applicability of the *Airborne System* is broad and circumvents limitations associated with chip-based analytical systems, such as adsorption of the analytes or optical interferences at the walls of the sample containers. Furthermore, the low attomole detection limit highlights the potential of the method.

Dysfunctional adipocytes and insulin-producing pancreatic β-cells are dynamic parts in the development of type 2 diabetes. The mechanisms involved are however not yet fully understood. With this project we aim to give our contribution for the understanding of the phenomena associated with the development of the disease and at the same time provide science with new tools which can be useful in the pursuit of new knowledge, as well as in the development of novel drugs, both in type 2 diabetes or in other metabolic diseases.

The system was here applied in cellular studies at the single/few cell level. Reagents are added to the droplet using flow-through dispensers, with no physical contact with the droplet. After exposure of the cells to drugs, activators or inhibitors, the cell response (or lack of response) is monitored using fluorescence imaging detection and MALDI-TOF-MS.

Adipocyte lipolysis was followed. Stimulation of lipolysis with isoprenaline resulted in a pH decrease detectable by this methodology. Moreover, the addition of insulin resulted in the inhibition of isoprenaline stimulated lipolysis in adipocytes in the levitated droplet. The addition of glycated insulin to an adipocyte containing droplet revealed not to be as effective to stop lipolysis as non-glycated insulin, which is an important finding in the search for new targets in type 2 diabetes related research.

Additionally, we are now attempting to develop techniques which can interrogate and monitor analytes of interest in a levitated droplet, non-destructively, on-demand, and over extended periods of time and in real-time by MS. In current work

droplet fission is induced by polarization in a containerless environment. Various electrode configurations are attempted varying parameters such as number and shape, voltage, pulse length and frequency for the applied electric field in order to get the proper droplet response.

Miniaturization and single-cell analysis could ultimately result in a decreasing of the number of animal trials necessary in medical research.

Resumo

Inovações em biomedicina e áreas relacionadas exigem o paralelo desenvolvimento de novos métodos analíticos. Assim, a técnica aqui apresentada é baseada na levitação acústica de pequenas amostras. O estudo de reacções intra e extracelulares utilizando apenas uma ou poucas células é, desta forma, possível. Microambientes adequados ao estudo the específicos tipos celulares e respectivas reacções podem assim ser criados, funcionando como sistemas biomiméticos.

As aplicações do *Airborne System* são variadas. Com esta técnica algumas limitações, tais como a adsorção dos analitos e interferências ópticas devido à presença de superficies, associadas com outras técnicas de miniaturização incluindo as que se baseiam no uso de chips, são eliminadas. Além do mais, a possibilidade de detecção ao nível da attomole aumenta ainda mais o potencial desta técnica.

Adipócitos disfuncionais bem como as células produtoras de insulina – células β - são factores importantes envolvidos no desenvolvimento da diabetes tipo 2. No entanto, estes mecanismos não são ainda totalmente conhecidos. Com este projecto pretendemos contribuir para a compreensão dos fenómenos associados com o desenvolvimento da doença e ao mesmo tempo equipar a ciência com novas ferramentas que poderão ser úteis, quer na descoberta quer no desenvolvimento de novas drogas para o tratamento, não só, da diabetes tipo 2, como de outras doenças metabólicas.

O *Airborne System* foi aqui aplicado no estudo do metabolismo dos adipócitos ao nível de uma/poucas células. Os reagentes são adicionados à gota levitada usando *flow-through dispensers*, sem qualquer contacto físico. Depois de expostas tanto a drogas activadoras como inibitórias, a resposta das células (ou a falta dela) é monotorisada usando *fluorescence imaging detection* e MALDI-TOF-MS.

A estimulação da lipólise em adipócitos é feita através da adição de isoprenalina. A resultante diminuição dos valores de pH do meio pode ser então detectada com o uso desta metodologia. A inibição da lipólise iniciada com a administração de isoprenalina foi conseguida através da adição de insulina. Em paralelo, a administração de insulina glicada, revelou não ser tão eficaz no objectivo de parar a lipólise, como foi a insulina não glicada. Este facto representa uma descoberta importante na procura de novos caminhos que levem ao total conhecimento dos mecanismos responsáveis pelo desenvolvimento da diabetes tipo 2.

Ainda, estamos no momento a aplicar esforços no desenvolvimento the técnicas que nos permitam seguir a resposta das células de forma não destrutiva, por longos períodos de tempo e em tempo real utilizando MS. Actualmente, a fissão da gota levitada é induzida através da polarização de cargas num ambiente em que não existe qualquer contacto da gota com superficies externas. Eléctrodos com várias configurações são testados, fazendo variar parâmetros tais como o valor e o perfil da voltagem aplicada, frequência e comprimento dos pulsos aplicados no campo eléctrico, de forma a conseguir uma resposta apropriada por parte da gota em levitação.

O desenvolvimento desta técnicas analítica poderá, em última análise levar a uma diminuição do número de animais sacrificados diáriamente em laboratório.

Abbreviations

MS	Mass Spectrometry
MALDI	Matrix Assisted Laser Desorption and Ionization
TOF	Time of Flight
ESI	Electrospray Ionization
CID	Collision Induced Dissociation
ATP	Adenosine Triphosphate
cAMP	Cyclic Adenosine Monophosphate
PKA	Protein Kinase A
PKC	Protein Kinase C
K^+-ATP Channels	ATP Sensitive K^+ Channels
GLUT4	Glucose Transporter 4
Ach	Acetylcholine
FFA	Free Fatty Acids
SNS	Sacral Neuro Stimulation
β-AR	β-adrenergic receptor
AC	Adenylate Cyclase
HSL	Hormone-Sensitive Lipase
TNF-α	Tumor Necrosis Factor α
PPARγ	Peroxisome-Proliferator Activated Receptor Gamma
IL-1/6/11/12/27	Interleukin 1/6/11/12/27
OSM	Oncostatin M
LIF	Leucemia Inhibitory Factor
CNTF	Ciliary Neurotrophic Factor
CT-1	Cardiotrophin
CHO	Chinese Hamester Ovary
PMT	Photomultiplier Tube
LED	Light Emitting Diode
NIR	Near Infrared
HPTS	8-Hydroxypyrene-1,3,6-Trisulfonic Acid

TFA	Trifuoroacetic Acid
DHB	2,5.dihydroxybenzoic acid
CHCA	α-cyano-4-hydroxybenzoic Acid
SA	Sinapinic Acid
BSA	Bovine Serum Albumine
IP_3	Inositol Triphosphate
HAc	Acetic Acid
AGEs	Advanced Glycation End Products
ELISA	Enzyme-Linked Immunosorbent Assay
FAIMS	Field-Asymmetric Ion Mobility Spectrometry

Keywords

Acoustic levitation
MALDI
HPTS
Type 2 diabetes
Adipocytes
Insulin
Single-cell
Cell-cell comunication
Miniaturisation

Submitted Publications and Communications

I. Santesson, S.; Degerman, E.; Rorsman, P.; Johansson, T.; Lemos, S.; Nilsson, S. Cell-Cell Communication between Adipocytes and Pancreatic β-Cells in Acoustically Levitated Droplets, Integrative Biology, 2009, DOI:10.1039/b907834g;

II. Lemos, S.; Gustavssson, N.; Degerman, E.; Eliasson, L.; Nilsson, S. Interfacing Airborne Cell Chemistry with MALDI-TOF-MS, Lab on a Chip, 2009 (Submitted);

III. Part of the present work was presented in Pittcon 2009 in Chicago.

Contents

The thesis under the title:

Acoustic “Wall-Less” Test Tubes for Cell Biology in Type 2 Diabetes Related Research

Was elaborated by:

Sandra Lemos, M2781,
Master student of Biochemistry in Universidade da Beira Interior.

With basis on the work developed within the period 2008/09-2009/07 at Lund University, Lund Institute of Technology, Department of Pure and Applied Biochemistry, where temporarily got the identification number 831208-P188.

Under the supervising of:

Prof. Staffan Nilsson, professor at Lund University, Lund Institute of Technology, Department of Pure and Applied Biochemistry;
Prof. Ana Cristina Cabral, professor at Universidade da Beira Interior, Health Sciences Research Center.

Presented at the Department of Health Sciences, Universidade da Beira Interior, at 10.00 a.m. on the 7th of September, 2009, with the purpose of reaching the master degree.

1. Introduction

Many problems in bioanalytical science are associated with scarcity of biological material. Often, samples of interest are rare in nature or hard to produce in big scale, whether this is due to low abundance or to very high extraction and purification efforts. Enzymes and some proteins, for example, are often very expensive and living human cells usually very hard to get in large amounts due mainly to ethic reasons[1].

Today, only few analytical systems combine high sample throughput with the ability to extract high quality information from particular biological and biochemical events. In an effort to overcome these limitations, a wall-less test tubes system - the "Airborne System" - has already been developed[2,3]. In this way, sample loss by adsorption to container walls is avoided, as well as sample contamination, which has special relevance when dealing with these small amounts of material.

The airborne system coupled with fluorescence imaging detection and Matrix-assisted laser desorption/ionization time of flight mass spectrometry (MALDI-TOF-MS), provides the analysis of single cells responses, cell-cell communication, and specific mixed cell populations in Real-Time and combined with high resolution analysis. These methodologies offer the opportunity to study responses in different cell systems and how different stimuli/inhibitors affect them.

.

1.1 Diabetes

Diabetes affects over 150 million people worldwide and this number is expected to double by 2025[4]. People with diabetes have large reductions in life expectancy and in quality of life due to diabetes-specific microvascular complications in the retina, renal glomerulus, and peripheral nerve, and to extensive atherothrombotic macrovascular disease affecting arteries that supply the heart, brain, and lower extremities. It has been estimated that up to 70% of patients with acute myocardial infarction have either diabetes or impaired glucose tolerance[5].

The global epidemic of type 2 diabetes goes hand in hand with a global epidemic of obesity (more than 90% of the type 2 diabetes patients are also obese), already termed globesity by the world health organization.

1.1.1 Type 2 Diabetes, Glucotoxicity, Glucose Intolerance and Insulin Resistance

Both genetic and environmental factors (mainly obesity) contribute to insulin resistance[6]. Insulin resistance induces a compensatory increase in β-cell mass, which in many people results in normal glucose levels. In other people, intrinsic defects in this compensatory β-cell response prevent adequate compensation, and impaired glucose tolerance or type 2 diabetes occurs.

Recently, adverse effects of hyperglycemia on insulin target tissues and on pancreatic β-cells have also been recognized, and this phenomenon has been termed "glucotoxicity." Chronic hyperglycemia has been shown to induce multiple defects in β-cells, including early decreases in glucose-stimulated insulin secretion, and late irreversible changes in insulin-gene transcription and β-cell mass[7]. In patients with impaired glucose tolerance, lowering of glucose levels dramatically reduces the progression to type 2 diabetes[8], suggesting that glucotoxicity plays a major role in this transition.

Recent work with tissue-conditional knockouts of both Glut4 and the insulin receptor in mice have shown that adipose tissue plays a central role in the pathogenesis of insulin resistance, and that there is significant cross-talk among insulin target tissues[9].

1.1.1.1. Glycation of Insulin

Hyperglycemia is one of the primary symptoms of diabetes and consequently the post-translational non-enzymatic glycation of both structural and functional proteins with excessive glucose occurs under hyperglycaemic reducing conditions[10], such as glucose-6-phosphate dehydrogenase, aldehyde reductase, hemoglobin and the most important β cell protein, insulin[11]. The glycation rate and extent depend on the glucose concentration and the time exposure to glucose.

The glycation involves the reaction between the aldehyde group of the reducing glucose and the free amino group of the protein and the subsequent rearrangement of the producing labile Schiff base to form the stable Amadori product (Ketoamine)[12,13] as shown in figure 1. The Amadori products very slowly undergo a series of rearrangement, dehydration and inter- as well as intramolecular cross-linking reactions to form yellow-brown, fluorescent and cross-linking substances, called advanced glycation end products (AGE)[14].

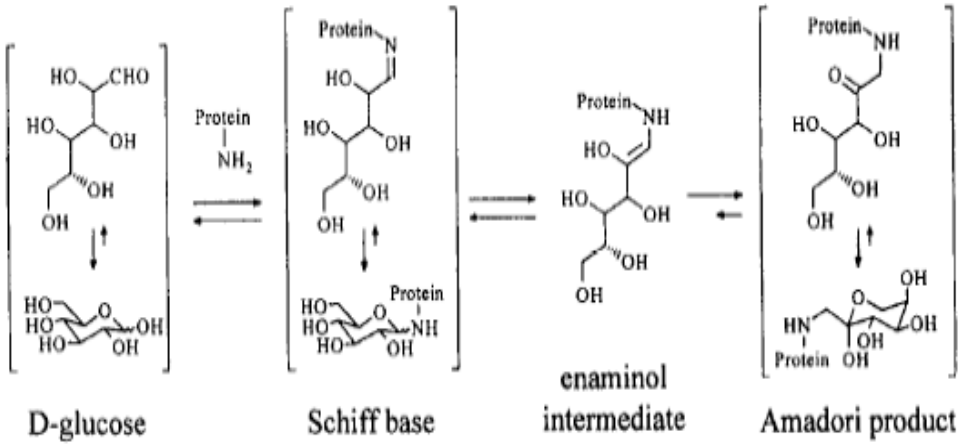

Figure 1. Formation of the glucose-protein Schiff base and the Amadori rearrangement.

When isolated Langerhans islets and clonal pancreatic β-cell line were cultured in high glucose medium, they contained higher concentration of glycated cellular insulin that could be readily secreted as a response to a variety physiological

stimulator[15]. The mechanism of glycation in the β-cell was suggested that it probably started after the transporting of glucose into the β-cell and rapid metabolism of glucose by glucokinase to a reactive glycating agent, glucose-6-phosphate[15].

The product of glycation is stored in the secretory granules in pancreatic β-cells prior to the co-secretion with insulin[15]. The secretion of glycated insulin occurs in both the early first-phase and the later second-phase, the same as the native insulin secretion. The early secretion might partly reflect a neurally mediated secretory response and the second-phase secretion might be analogous to the physiological insulin response[16].

The N-terminal Phe^{1} residue of the B-chain had been revealed to be the only glycation site of human insulin by enzymatic digestion combined with electrospray tandem MS[10]. While in contrast, the N-terminal Gly^{1} of A-chain and N-terminal Phe^{1} of B-chain were shown to be the sites of glycation in novel naturally occurring diglycated insulin[17,18].

The glycated insulin is less effective in regulating plasma glucose homeostasis and has a negative affect on lipogenesis observed on mice. Less effective ability of glycated insulin to stimulate glucose oxidation had been also studied in the isolated mouse diaphragm muscle[12,13]. The presence of increased concentrations of circulating glycated insulin in human with type 2 diabetes and the impaired activity has been studied using specific radioimmunoassay[19] and euglycemic-hyperinsulinemic clamp technique. No difference was observed between glycated and native insulin in receptor binding to CHO-T cells transfected with human insulin receptor and in vivo metabolic clearance[11].

The decreased biological activity coupled with glycated insulin resulted in the glucose toxity and pancreatic β-cell dysfunction[12,13,15]. The glycation of insulin could lead also to a prolonged half-life with exacerbation of hyperinsulinaemia and insulin resistance[15]. Hence hyperglycemia had been suggested to be a cause as well as a consequence of β-cell dysfunction and insulin resistance in type 2 diabetes.

1.2. β-cells and Insulin Release Control

β-cells are the ones responsible of production and release of insulin, a hormone that regulates long term food intake and controls the level of glucose in the blood.

Although β-cells are specialized in fuel sensing to adjust insulin secretion according to variations in the plasma concentration of glucose and other nutrients, they are also subject to a major neurohormonal control[20,21].

During meals, insulin secretion induced by absorbed nutrients is augmented by intestinal hormones (incretins), among which glucagon-like peptide 1 (GLP-1) plays a dominant role, and by acetylcholine (ACh) released by parasympathetic nerve endings in the islets. Accordingly, besides glucose, numerous agents can increase insulin secretion *in vitro*. They are traditionally categorized as initiators or primary stimuli when they are able to increase insulin secretion in the absence of any other stimulatory agent, and as potentiators or secondary stimuli when they are ineffective alone but increase insulin secretion in the presence of an initiator, particularly glucose. Hormones and neurotransmitters are not initiators; they have no effect on secretion when used alone. Thus, a small decrease in plasma glucose lowers the rate of insulin secretion by attenuating both the genuine effect of the sugar and the effectiveness of non-glucose stimuli. Conversely, *in vivo*, small postprandial increases in plasma glucose may result in larger insulin responses than those expected from dose–response curves defined *in vitro* because of the interaction with non-glucose stimuli whose action is also amplified[22].

However, the mechanisms by which the different potentiators exert their effects are variable.

1.2.1. Stimulation by Acetylcholine

Acetylcholine (ACh) increases $[Ca^{2+}]i$ in β-cells by two major mechanisms: an IP_3-mediated mobilization of Ca2+ from the endoplasmic reticulum and a Na^+ mediated depolarization enhancing Ca^{2+} influx through voltage-dependent Ca^{2+} channels[21]. ACh thus increase the triggering signal through mechanisms that are completely independent of an action on K^+-ATP channels. It also markedly activates amplifying pathways

distinct from that operated by glucose. The production of diacylglycerol by ACh activates PKC, which also sensitizes the exocytotic machinery to the stimulation by Ca^{2+} [23]. The contribution of the amplifying pathway in insulin secretion with ACh is clearly greater than that of the change in $[Ca^{2+}]_i$[21]. It has been reported that combined pharmacological activation of PKA and PKC suffices to induce insulin secretion even when $[Ca^{2+}]_i$ in β-cells is very low, suggesting that protein kinases could substitute for Ca^{2+} as triggering signal[24]. Physiologically, the hierarchy between the triggering signal (the $[Ca^{2+}]_i$ rise) and amplifying signals sensitizing to the action of Ca^{2+} is respected by hormones and neurotransmitters. The increase in insulin secretion brought about by ACh is tightly glucose-dependent.

1.3. Adipose Tissue

Adipose tissue is an interesting organ that is in constant communication with other tissues via adipokines, lipid factors and lipoprotein particles and exerts a profound impact on whole-body metabolism. Changes in free fatty acid concentration and flux affect other cell types, such as pancreatic β-cells.

1.3.1. Lipolysis

Lipolysis is the breakdown of fat stored in fat cells. Triglycerides undergo lipolysis (hydrolysis by lipases) and are broken down into glycerol and fatty acids. During this process, free fatty acids (FFA) are released into the bloodstream and circulate throughout the body.

The concentration of FFA in plasma is the result of a balance between lipolytic production, the uptake by the liver and the oxidation by muscle, heart, liver, and other tissues[25].

1.3.1.1. Regulation

The SNS is the main promoter of lipolysis in humans, and insulin the major antilipolytic hormone. The proposed mechanism for stimulation and inhibition of lipolysis in adipocytes is schematically showed in Figure 2.

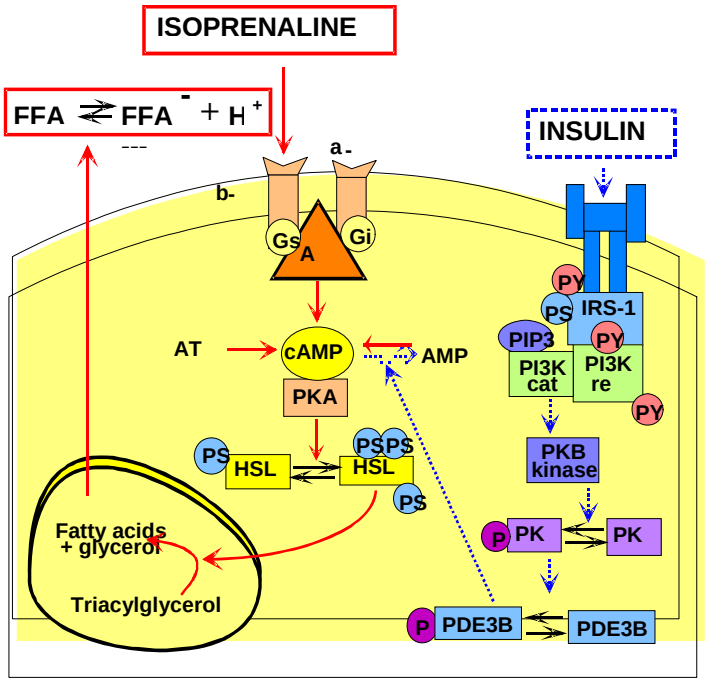

Figure 2. Stimulation and inhibition of lipolysis in adipocytes[26].

1.3.1.1.1 Inhibition

Insulin signalling is mediated by a complex, highly integrated network that controls several processes[27]. In adipocytes, the insulin released by the β-cells leads to inhibition of lipolysis and enhances lipid storage. Stimulation of the β-adrenergic receptor (β-AR) with β-adrenergic agonists results in activation of adenylate cyclase (AC), production of cAMP and activation of cAMP dependent protein kinase (PKA). PKA phosphorylates hormone-sensitive lipase (HSL), leading to activation of the enzyme and increased lipolysis giving extracellular release of free fatty acids (FFA). The signalling pathway from the insulin receptor (IR) to phosphodiesterase (PDE) 3B involves phosphatidylinositol 3-kinase (PI3K) with protein kinase B (PKB) mediating the PI3K dependent phosphorylation and activation of PDE3B that in turn lowers cAMP[28].

Adenosine is another lipolysis inhibitor that has a Gi protein coupled receptor in the adipocyte. In this way, basal lipolysis is normally inhibited by endogenous

adenosine spontaneously produced by the adipocyte. An activation of lipolysis may take place through TNFα mediated decrease of Gi concentration coupled to adenosine receptor which blocks the continuous lipolysis inhibition signal[29].

1.3.1.1.2. Stimulation

The following hormones induce lipolysis: isoprenaline[30], epinephrine, norepinephrine, glucagon and adrenocorticotropic hormone.

The activation of Gs protein is the best-known mechanism that mediates lipolytic activation. Catecholamines, adrenaline and noradrenaline and isoprenaline are the paradigm of this group of hormones. They have three subtypes of β-receptors and two subtypes of α-receptors. The positive regulation of lipolysis by catecholamines using the Gs/AC/PKA/HSL pathway involves β1, β2 and β3-AR. The three β-receptors are coupled to a Gs-protein, they transmit an activation signal to adenylyl cyclase (AC) increasing cAMP production. Then a cAMP-dependent protein kinase (PKA) is activated and this finally leads to phosphorylation and activation of HSL and perilipin A[31]. HSL breaks the triglycerides stored in adipocytes thus producing glycerol and FFA.

1.3.1.2 Fuel Partitioning

Although animals go through feeding/fasting cycles, the liver maintains a relatively constant fatty acid flux into triglyceride biosynthesis[32]. During fasting, the free fatty acid is derived from lipolysis of adipose tissue triglyceride, is transported to the liver and is re-esterified to form hepatic triglyceride. The partitioning of lipids between adipose tissue and other tissues plays an important role in insulin signaling and cellular viability. Adipose tissue is specialized for triglyceride storage and has a very high capacity to accumulate triglycerides. Thus, the enhanced lipolysis and consequent free fatty acid flux from adipose tissue in obesity exposes other tissues to a substantial fatty acid burden[33].

Obesity is associated with changes in adipocyte gene expression spanning many pathways. These changes alter fuel partitioning between adipose tissue and other tissues.

1.3.2. Obesity and Type 2 Diabetes

Obesity is an increasing problem, with more than one billion people worldwide classed as overweight and at high risk for developing other serious conditions, such as heart disease and diabetes. There is a strong and consistent association between obesity and the development of type 2 diabetes (fig. 3).

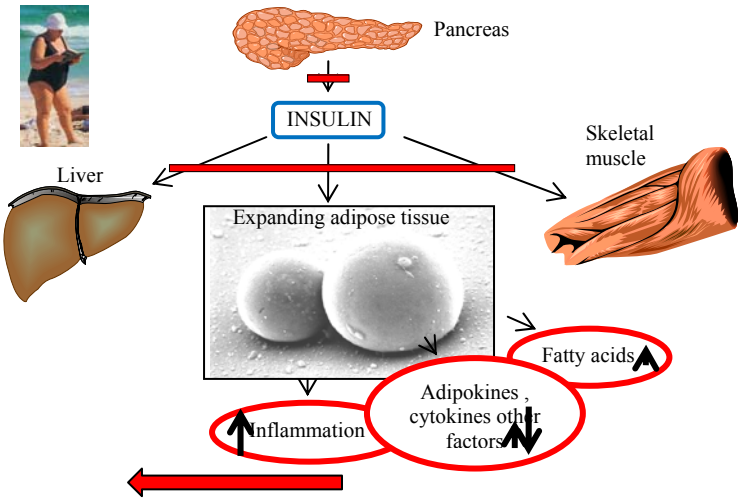

Figure 3. Links between obesity and the development of T2D.

The unbalance on FFA and glucose plasma levels are closely related to obesity, insulin resistance, dyslipidaemia and type 2 diabetes mellitus. It has been proposed that chronically elevated FFA concentrations may reduce insulin secretion in type 2 diabetes[34]. These FFA-related disturbances are referred to as lipotoxicity[35]. However, it is important to point out that current evidence argues against triglyceride itself being the reason of these fatty acid-mediated actions. Rather, strong evidence supports a role for diacylglycerol in the blunting of insulin signaling. Increased expression of

diacylglycerol acyl transferase improves insulin sensitivity[36] whereas inhibition of diacylglycerol kinase suppresses insulin signaling[37].

Additionally, adipose tissue releases non-esterified fatty acids, glycerol, hormones, proinflammatory cytokines and other factors which appear to be released in altered amounts in obese individuals which is correlated with the development of type 2 diabetes[38]. The role of inflammation in obesity has gained attention, beginning with the discovery that the macrophage content of adipose tissue in obese humans and rodents increases dramatically[39].

As more evidence emerges, there is a stronger case for targeting adipose tissue in the treatment of type 2 diabetes. In an interesting study, Kahn and colleagues bred mice to lack the insulin receptor in their fat cells[40]. These animals had a lean body mass and differed from control mice in that they were protected from obesity associated with age or overeating. Importantly, they were also protected from developing obesity-associated or age-related insulin resistance, which leads to diabetes. Interestingly, these mice had two different populations of adipocytes, small and large, which differ in expression of the enzyme fatty-acid synthase and other transcription factors. It is thought that loss of the adipocyte insulin receptor unmasks differences between two sizes of fat cell and that the small adipocytes are somehow protected against excessive fat loading, preventing the mice from becoming obese. Although these mice showed insulin resistance in the adipose tissue, whole-body glucose metabolism was not affected.

In another perspective, peroxisome-proliferator activated receptor gamma (PPARγ) agonists, for example the thiazolidinediones, redistribute fat within the body (decrease visceral and hepatic fat; increase subcutaneous fat) and have been shown to enhance adipocyte insulin sensitivity, inhibit lipolysis, reduce plasma FFA and favourably influence the production of adipocytokines[35].

.

1.3.2.1. A Matter of Size

There are reports indicating an association between enlarged fat cells and the development of Type 2 diabetes[41]. For example, in enlarged fat cells, lipid metabolism has been shown to be disturbed leading to increased hydrolysis of stored triglycerides

(lipolysis)[35]. However, it has also been suggested that insulin resistance in obese patients is associated with an increased number of small adipose cells with decreased expression of differentiation markers[42,43] and subnormal ability to sequester and store fat. Thus, reduced ability to recruit new adipocytes to store excess energy may result in the storage of triglycerides in other cells contributing to the development of Type 2 diabetes. Regarding the relative importance of adipocyte number and size, respectively, in the development of obesity, there has been some controversy. A recent study reports that adipocyte number is the major determinant for fat mass in adults and that the number of fat cells stays constant in adulthood in lean and obese individuals, even after marked weight loss, indicating that the number of adipocytes is set during childhood and adolescence[44].

1.3.2.2.Adipose Tissue inflammation

The obesity-associated increased infiltration of immune cells, especially macrophages, is well-established[45]. The recruitment of macrophages from the blood to the adipose tissue in obesity leads to an inflamed condition, culminating in the deregulation of the synthesis and release of adipocyte derived hormones, which are, in some cases, associated with decreased insulin sensitivity. Excess adipose tissue contributes to systemic inflammation and targeting inflammation is an attractive approach for the treatment of insulin resistance.

The first molecular link identified between inflammation and obesity was TNFα (tumor necrosis factor alpha)[46]. Thus, it has been demonstrated that over-production of TNFα in adipose tissue is an important feature of obesity and contributes significantly to the development of insulin resistance. Many other inflammatory mediators have now been shown to exhibit patterns of expression and/or impact on insulin action in a manner similar to TNFα, especially increased levels of interleukin (IL)-6 has been linked to insulin resistance and type 2 diabetes[47]. The IL-6 family of cytokines include IL-6, IL-11, IL-27, oncostatin M (OSM), leucemia inhibitory factor (LIF), ciliary neurotrophic factor (CNTF), cardiotrophin-1 (CT-1) and cardiotrophin-like cytokine (fig. 4).

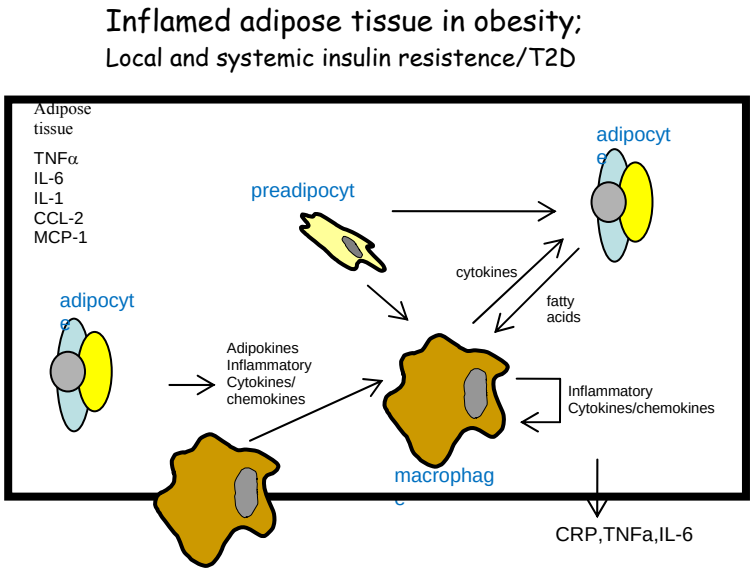

Figure 4. Inflamed adipose tissue in obesity.

These cytokines are characterized by their common use of the gp130 receptor (β-subunit) as a signaling subunit[48]. In addition, the IL-6 family members also have cytokine specific receptor components (α-receptors). The α-receptors for IL-6, IL-11 and CNTF can also be found in a soluble form and these soluble receptors can bind their ligands in a manner identical to their membrane-associated forms. These soluble receptors have the unusual potential to confer cytokine responsiveness to cells expressing gp130 that do not express the membrane–associated forms of the α-receptors (trans-signaling). This specific agonistic mechanism has been shown to be pathogenic in several chronic inflammatory diseases.

A reduction of local inflammation in adipose tissue, either through pharmacological intervention or through genetic manipulation of pro-inflammatory pathways, is invariably associated with improvements in local and systemic insulin sensitivity[49]. While inflammatory pathways are the ultimate mediators of insulin resistance, other events in adipose tissue may precede the initiation of inflammation-induced adipose tissue dysfunction[49].

1.3.2.3. Leptin, Adiponectin and Resistin

Leptin, adiponectin and resistin are hormones produced by the adipose tissue which are thought to be connected to the development of insulin resistance and type 2 diabetes.

Leptin plays a profound role in fuel partitioning. Diet-induced obesity simultaneously leads to increased leptin secretion and a blunting of the autocrine leptin signal in adipocytes. The leptin signal tends to be anti-adipogenic, a conclusion that emerged from the protection from obesity afforded to transgenic mice overexpressing the leptin β-receptor in adipocytes[50]. Functionally, the net result is comparable to states of partial or complete lipodystrophy; *i.e.* excess triglycerides accumulate ectopically in tissues such as liver, muscle, and β-cells, where they contribute significantly towards the lipotoxic effects of lipids.

Additionally, the levels of adiponectin were found to be reduced in diabetics compared to non-diabetics, playing a role in the suppression of the metabolic derangements that may result in the disease[51]. Moreover, a mouse obesity model that over-expresses the adipocyte-derived circulating factor adiponectin was described[52]. These mice retain adiponectin levels at concentrations found in a lean mouse. Under these conditions, the mice further expand their adipose tissue mass quite dramatically. Surprisingly, despite the mutation and the huge excess of adipose tissue, these mice have a fairly good metabolic profile and retain near normal insulin sensitivity, a normalized lipid profile and hallmarks of a significant improvement in adipose tissue histology. An increased number of smaller fat cells is apparent, with a reduced infiltration of macrophages. As a result, insulin sensitivity is preserved.

It is believed that there are positive correlations between resistin levels and insulin resistance[53,54]. Resistin has been shown to increase transcriptional events leading to an increased expression of several pro-inflammatory cytokines including interleukin-1 (IL-1), interleukin-6 (IL-6), interleukin-12 (IL-12), and tumor necrosis factor-α (TNF-α in an NF-kB-mediated fashion[55,56]. Because resistin is reputed to contribute to insulin resistance, results such as those mentioned suggest that resistin may be a link in the well-known association between inflammation and insulin resistance[57].

1.4 Acoustic Levitation

The interest aroused by microtechnology and nanotechnology in chemical, biochemical, pharmaceutical, biological, biomedical, biotechnological fields, among others, is indisputable. Often the amount of sample available is small and/or the sample is expensive requiring the corresponding miniaturization of analytical instrumentation[58], i.e., lab-on-a-chip systems. Recent breakthroughs in miniaturized analytical instrumentation include fully integrated ''lab-on-a-chip'' and micro total analysis systems[59]. However, it is inherently difficult to handle small samples with volumes in the range of nano-to-microliters. At present, chip-based analytical systems are subject to major shortcomings, such as the risk of analyte adsorption on walls and at interfaces which is especially high in miniaturized analytical systems and optical interference at the walls of chips that hampers detection[60]. In this context, acoustic levitation is an interesting and useful containerless sample handling method for suspending small solid, liquid and even gaseous samples, which are usually suspended in a gaseous environment like air by means of a stationary ultrasonic field[60-62]. Absorption and contamination processes from solid walls or other external objects, or between samples are strongly suppressed by this procedure[60].

Acoustic levitation constitutes an efficient tool for sample handling in both developing different steps of the analytical process and process monitoring[59]. This all justifies a call for attention to this particular way of preparing miniaturized samples. However, more in-depth research on the fundamentals and equipment for implementation of this technique is required (namely, devices for sample and reagent delivery, ultrasound levitators, and units for transferring sample or aliquot to the detector and detection systems), as well as on current applications.

Currently, acoustic levitation is being applied for a variety of analytical and bioanalytical purposes[60] with a large number of different applications in bio-sciences[61], crystallization studies of proteins[63], evaporation processes[64,65], formation and analysis of surface layers[66] or polymerisation reactions[67]. In addition, levitation permits chemical pre-treatment steps such as enrichment, extraction, and derivatisation as well as combination with other analytical techniques such as optical spectroscopy[68]. However, few studies have focused on living cells[69], despite the potential usefulness of the airborne analytical system for such applications.

1.4.1 Fundaments of the Technique

The principles of acoustic levitation are extensively described elsewhere[70]. some complex theories of non-linear acoustics remain unclear[71]. It was first described by Bucks and Müller in 1933[72]. Its flexibility and potential in various fields is widely documented, mainly by studies in the analytical and bioanalytical fields[61,69].

This technique allows us to suspend droplets without any mechanical contact. Acoustic levitators usually operate at ultrasonic frequencies of 15–100 kHz (i.e. at wavelengths in the range 2.2–0.34 cm). A sonotrode emits an ultrasonic wave with a certain frequency (100 kHz in this work) which is reflected on a concave acoustic mirror. At this frequency droplets with diameters up to 1.7mm can be levitated, corresponding to approximately 3.5µL.

The reflector is adjusted concentrically with the reflector at a distance of a few multiples of half of the wavelength of the ultrasound. This distance can be easily defined by moving the reflector, which is connected to a micrometer adjuster screw. Solid or liquid samples with effective diameters of less than half the ultrasound wavelength under ambient atmospheric conditions can be levitated in each of these equally spaced pressure nodes of the stationary ultrasonic field due to axial radiation pressure and radial Bernoulli stress[71] as shown in figure 5:

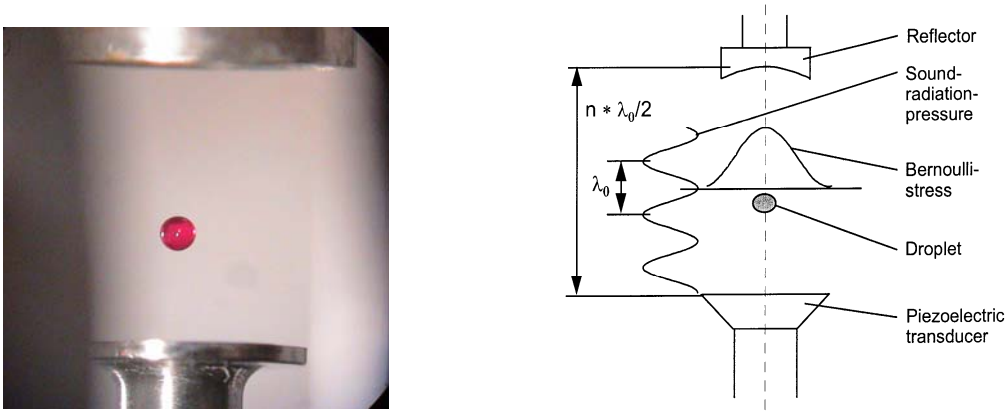

Figure 5: Fundaments of acoustic levitation.

Reflections between the sonotrode and the reflector generate a standing acoustic wave with a defined number of local nodes (Fig. 6).

Figure 6. 5 Local nodes of an acoustic standing wave made visible by levitation of small water droplets.

In this way, a sample can be held in a constant position for several hours. However, not all nodes are useful for stable levitation, those lying directly in front of the transducer and the reflector shall not be chosen[73]. Furthermore, with ultrasonic wavelengths above ca. 8 mm, the maximum volume of a levitated liquid drop cannot be determined as a function of the wavelength, as it is determined by the ratio of hydrostatic pressure to the capillary pressure generated by surface tension inside the drop. If this ratio, called the ''Bond number'', exceeds 1.5, then the drop will disintegrate. The two variables dictating the maximum volume of a levitated drop are therefore the surface tension and the specific density of the liquid[74,75]. With solids, the main requirement derives from the density of the material; however, the limits for this parameter depend on the particular acoustic levitator and are in the range 0.5–8 g/ml[60].

Acoustic levitation can as well be accomplished under microgravity conditions or in a liquid environment. Under microgravity conditions, a liquid sample can be positioned exactly at the pressure node, where the acoustic pressure and levitation force are both zero, whereas the acoustic velocity is maximal. Stable levitation is therefore possible at such a position[71]. Moreover, a cylindrical glass tube can be placed around the acoustic transducer and reflector in order to form a closed chamber, inside which the acoustic standing waves are generated. This type of adaptation enables accurate control of the temperature and the humidity inside the tube. A slight air flow can additionally be blown into the tube to control air humidity and sublimate concentration in the tube.

It should be mentioned that the samples do not need to have special physical properties like magnetic or dielectric moments unlike other types of levitation.

1.4.2 Sample Delivery

The importance of sample delivery is frequently ignored in studies on acoustic levitation, even though precision in analyses relies heavily on an appropriate choice of sample volume[59].

Delivery systems are closely related to the nature of the sample (liquid, suspension, solid or gas). Any type of system (e.g., micropipette, capillary, or microsyringe) can be used to position a drop from a liquid or slurry sample in an ultrasonic levitator (Figure 7). When the needle or tip holding the drop is positioned in the ultrasonic field, the amplitude must be raised in order to overcome the adhesion forces that attach the drop to the needle or tip[59]. Detaching the drop from a microsyringe tip can be facilitated by coating the tip with a hydrophobic substance (e.g., paraffin in n-hexane or silicone), provided it does not alter the sample composition; it is more difficult to detach the drop for liquids with a low surface tension and/or low viscosity. Thus, levitation of solvents, such as diethylether, is virtually impossible; by contrast, ethanol, methanol and toluene are readily detached because of their lower adhesion forces to the needle tip[59].

Figure 7. Detaching a droplet from a silicon coated capillary tip.

Capillaries can be coated with glass or polymers, but should be as thin as possible in order to reduce adhesion forces[61]. Also, the use of high-power ultrasound during sample positioning facilitates drop detachment; the droplet can be easily stabilized by adjusting the distance between the transducer and the reflector, and setting

an appropriate ultrasonic power[60]. The microsyringe has so far proved to be the best choice of delivery system in terms of precision, which is about ±0.05µl[76].

One other option for a non-contact delivery device is an in-house-developed piezoelectric flow-through droplet dispenser[77,78] (Figure 8). This device features high precision, a wide range of droplet size (up to picoliter volumes, which is of interest for miniaturization purposes), high frequency for droplet ejection (up to 9 kHz) and the capability to dispense samples from a flowing liquid (e.g., in a flow-injection system). In this way, a number of microdroplets can be accumulated until the desired droplet size is reached [79].

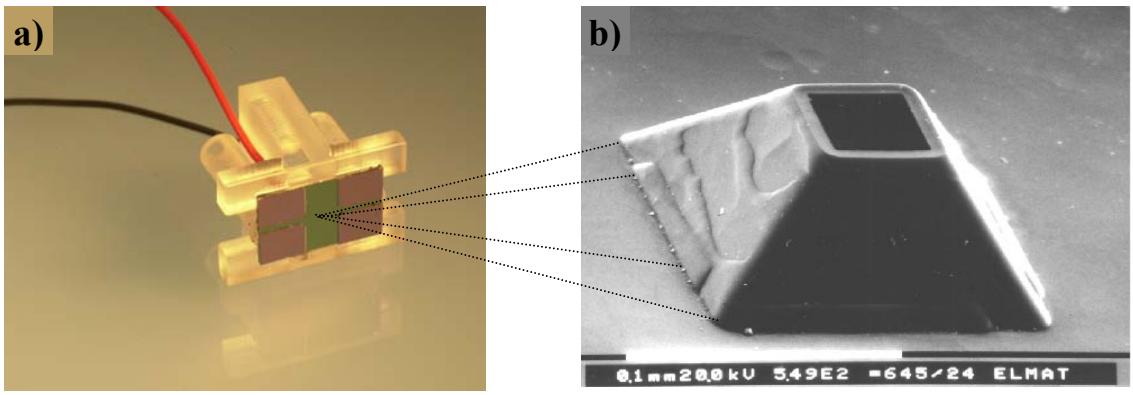

Figure 8. a) The flow-through droplet dispenser; **b)** Close up of the nozzle.

The flow-through droplet dispensers are fabricated using silicon micromachining. Droplets are ejected from a flow-through channel formed by joining two microstructured silicon plates with a protruding pyramid-shaped nozzle in the centre of the channel and a multilayer piezoelectric element connected to a push-bar in the channel wall opposite the nozzle (Figure 9.a). By applying a short voltage pulse across the piezoelectric element, this is elongated and pushed into the channel, thereby generating a pressure pulse in the liquid, the increased pressure accelerating the liquid in the nozzle causing the ejection of a droplet as a result (Figure 9.a,b,c). This process can be repeated over a frequency range of up to several kHz.

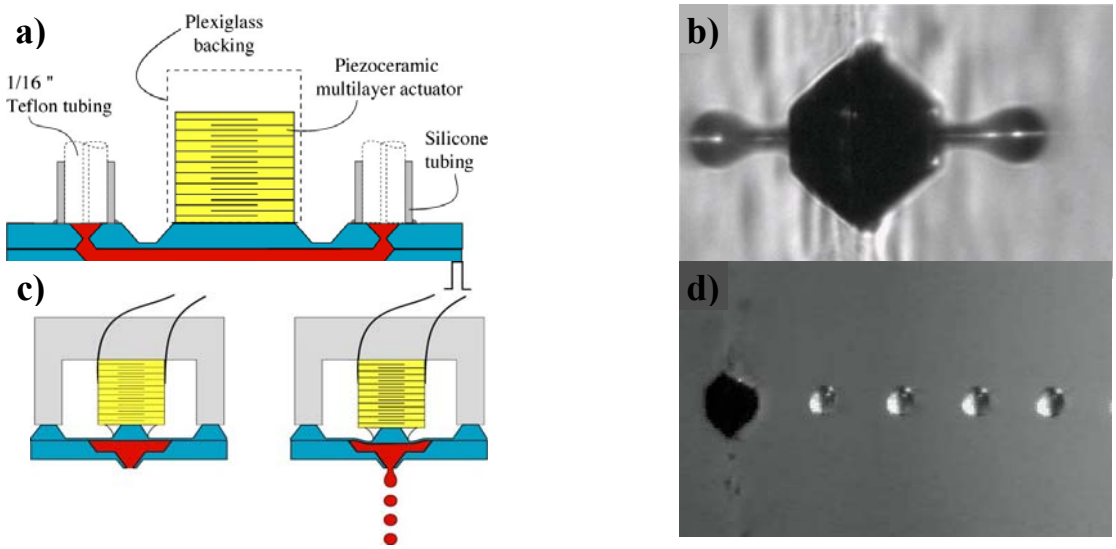

Figure 9. a) Schematic description of the flow-through dispenser; **b), c), d)** Illustration of the droplet ejection process.

The volume of the ejected droplet, typically in the range 40–100 pl, depends on the size of the nozzle, the shape of the voltage pulse and various liquid parameters, such as surface tension, viscosity and density. There is a viscosity limit for liquids to be ejected by the dispenser, and that depends on the nozzle dimensions. Thus, liquids of viscosity higher than the dispenser limit exhibit poor accuracy in droplet formation and volume; however, this problem can be overcome by heating the dispenser to a maximum temperature of 100ºC, which is imposed by the particular constituent material of the dispenser. Dispensing highly concentrated salt solutions can also cause problems due to salt crystallization in the nozzle, which can be avoided by using a dispenser furnished with a second layer of a salt-free liquid to cover the primary liquid upon ejection.

The dispenser has recently be used for cell additions[1]. In a similar perspective, Bolands group used a computer printer and an ink cartridge for encapsulating CHO cells and rat embryonic motoneurons, which were subsequently printed as ink onto ''biopapers'' made from soy agar and collagen gel. Cell viability was higher than 92% which indicates that mammalian cells can effectively retain their vital functions after delivered by this modified thermal inkjet printer[80]. More recently, Demircis group have developed a sophisticated nozzleless technology for encapsulating single to few cells

using an acoustic field. Mouse embryonic stem cells, fibroblasts, AML-12 hepatocytes, human Raji cells and HL-1 cardiomyocytes have been encapsulated in acoustic picolitre droplets of around 37 μm in diameter and ejected at high throughput levels (up to 10 kHz). Cell viabilities of over 89.8% across various cell types were reported[81].

One advantage of the flow-through microdispenser is that droplet evaporation can be accurately controlled by adding a solvent in order to keep the droplet volume constant, which is essential for quantification. This means using a system, such as an imaging detector, to monitor the droplet volume continuously in order to determine the evaporation rate during acoustic levitation.

1.4.3 Applications and Detection Techniques

Many analytical steps can be implemented in an ultrasonically-levitated drop, including concentration by evaporation[82], liquid–liquid extraction[61], gas-liquid extraction[79], biochemical derivatization[83], titration[73] and solvent exchange[61]. Levitation has also attracted substantial interest for protein crystallization, as the growth of suitable protein crystals is an essential step in the determination of protein structures by X-ray crystallography. At present, crystals are mostly grown using trial-and-error procedures, which waste large quantities of valuable material; this can be avoided by using acoustically-levitated drops in protein-precipitation studies for crystallization to establish the nucleation conditions resulting in the minimum possible consumption of protein material. Attempts in this direction have been made by using levitated drops of protein at a given concentration injected with crystallizing agents and monitoring the crystallization process by right-angle light scattering[63]. Another bioanalytical application is the development of miniaturized biospecific affinity two-phase partitioning in an acoustically-levitated drop[84]. This miniaturized method could also be used for separation of biologically-active membranes or organelles from individual cells for analysis.

One additional advantage of acoustic levitation for sample handling is the ability to perform detection in situ in order to expedite the analytical process and continuously monitor the effects of various processes on the levitating sample. The capabilities for detection in situ depend on the properties and operating conditions of the detection

system concerned. Thus, optical detectors are especially capable, as they can operate under remote, non-intrusive conditions. Various configurations involving diverse detectors have been developed for this purpose, one of which uses a CCD camera to record video images from the droplet in order to monitor the acoustic levitation process (e.g., deformations and other undesirable processes)[85].

Ordinary and intensified CCDs have also been used with other configurations, such as that for fluorescence imaging reported by Santesson *et al.*[69]. The main advantage of this configuration is that it enables dynamic processes to be monitored as well as quantifying analytes. Both native and indirect fluorescence can be used for monitoring or quantification of the target analytes. One example is the use of pH dependent fluorophores to measure the fluorescence resulting from a pH change depending on the analyte concentration[1].

Nilsson et al. used an Nd:YAG laser for the simultaneous measurement of elastic, fluorescence and phosphorescence signals from droplets in order to determine droplet diameter, temperature and species concentration[86]. The scattering signal is especially interesting on account of the wealth of information it can provide. One specific right-angle light-scattering detector comprises a microscope equipped with a CCD for continuous control of the drop volume. This detection technique is especially interesting for monitoring droplet processes [63].

Raman spectroscopy is another remote detection technique that has been successfully coupled to acoustic levitation. The approach allows quantification of analytes and the *in situ* study of dynamic processes, thus providing selective information for structural elucidation[85].

Acoustic levitation has been also coupled to SERS spectroscopy[87], photometry[63], fluorimetry[69], phosphorimetry[86] and X-ray diffraction techniques[88,89]. Further, it is possible to couple an ultrasonically levitated drop to separation techniques, such as capillary electrophoresis[82].

1.4.4. Advantages and Limitations

Sample levitation can be accomplished in different ways. Different levitation techniques include: magnetic, electrostatic, optical and aerodynamic. Comparison with this other levitation techniques emphasizes the advantages of ultrasonic levitation[59].

The main advantage of acoustic levitation above the others is that materials in different states of aggregation (solids, liquids, suspensions and gases) can be levitated by using acoustic forces irrespective of their physical properties, with the sole exception of the restrictions imposed by the density of the material[59]. Although ultrasounds can, in theory, be used to levitate any type of material,

The main disadvantages of acoustic levitation are acoustic streaming and non-uniformity in the force field. The energy-density distribution induces an acoustic convection flow that enhances heat and mass transfer, which can be an advantage or disadvantage with respect to stable positioning of samples as slight asymmetries in the acoustically induced convective flow field can result in undesired, uncontrolled sample rotation[59]. This situation is particularly important in applications where heat and mass transfer are decisive, especially with strong acoustic fields, so strict control of the field flow around an acoustically-levitated sample is extremely important[90,91]. A compromise solution must usually be adopted as the acoustic field should be strong enough to overcome gravity and prevent the drop from falling down, but not so strong as to cause the drop to disintegrate into small droplets under capillary forces, which are produced by the surface tension of the curved drop surface becoming too weak to keep the drop intact[75].

To consider is also evaporation of the solvent during levitation which gradually decreases the volume of the droplet and therefore increases the corresponding concentration of the solute[92,93]. This can although be used to overcome sample dilution by concentration through controlled droplet evaporation prior to detection.

1.4.5. The Airborne System

In 1997, Nilsson et al. reported the airborne system, which they used to develop analytical methods[94] and patented in 1999[95]. This system uses an APOS BA10 acoustic

levitator operating at a frequency of 100 kHz and temperatures of 0–70ºC. Although the optimal volume of a levitated droplet at a frequency of 100 kHz seemed to be between 500 nl and 1 µl, the maximum droplet volume tested was 2.3 µl and the minimum volume positioned in the levitator was 50 pl; however, the droplet evaporated almost immediately after positioning[96].

1.4.5.1. Airborne chemistry and living cells

The study of living cells and intracellular biochemical reactions in microdroplets is an interesting field for acoustic levitation, particularly in pharmaceutical, biological, and medical sciences. Improved knowledge of the chemical composition and dynamics of single cells should lead to better, broader understanding of how individual cells function in their natural environment.

1.5. Fluorescence Spectroscopy

There are a number of methods for generating contrast in optical imaging, but the most important approach is by far Fluorescence Spectroscopy.

Fluorometry is a method of chemical analysis in which a sample, exposed to radiation of one wavelength, absorbs this radiation and reemits radiation of the same or longer wavelengt; the intensity of reemited radiation is almost directly proportional to the concentration of the fluorescing material.

Fluorescence is a very sensitive technique which has seen a dramatic growth for use in cellular and molecular imaging. It permits a number of different molecules to be imaged in one specimen and allows a wide range of very specific structures and even species of molecules to be imaged. Fluorescence imaging can reveal the localization and enables measurements sometimes at the level of single-molecule detection[97]. Consequently, during the past years it has been a notable growth in the use of fluorescence in biological sciences. Fluorescence is nowadays a dominant technology used in biotechnology[98], flow citometry[99], medical diagnosis[100], DNA sequencing[101] and genetic analysis[102], just to name a few. The following advantages are responsible for bringing fluorometry into frequent use:

- Fluorescence measurements are extremely sensitive;

- They can be performed in the remission mode; this is a particularly useful technique when studying turbid or inhomogeneous materials;

- Since fluorescence is emitted in all directions, the geometrical design of the device can be more flexible;

- Immobilisation of an indicator on polymeric supports should allow the construction of a pH-indicating sensor.

1.5.1. Origin

The term 'fluorescence' was used for the first time by George Gabriel Stokes in 1852[103]. The name was chosen due to the mineral fluorite, composed of calcium fluoride, which had a visible emission when illuminated with "invisible radiation" (UV radiation).

1.5.2. Phenomena of Fluorescence

Luminescence is the emission of light from any substance and occurs from electronically excited states. Luminescence is formally divided into two categories – fluorescence and phosphorescence – depending on the nature of the excited state. Fluorescence typically occurs from aromatic molecules[97]. It is based on the property of some molecules that when they are hit by a photon, they can absorb the energy of that photon to get into an excited state. Upon relaxation from that excited state, the same molecule releases a photon: fluorescence emission. The energy of the photon that is released is always lower than that of the photon that was absorbed. So the photon that excites the dye always has a smaller wavelength than the photon that gets emitted. This is the so called Stokes Shift.

1.5.2.1. Lifetime and Quantum Yield

The fluorescence lifetime and quantum yield are perhaps the most important characteristics of a fluorophore. Quantum yield is the ratio of the number of photons emitted to the number absorbed. Substances with the largest quantum yields, approaching unity, display the brightest emissions.

The differential quantum yield is given by:

$$\Phi(\lambda) = \frac{\partial x / \partial t}{q^0_{n,p}\left[1 - 10^{-A(\lambda)}\right]} \qquad (1)$$

Where:

- $\partial x / \partial t$ is the rate of change of a measurable quantity (spectral or any other property);
- $q^0_{n,p}$, the amount of photons (mol or its equivalent einstein) incident (prior to absorption) per time interval (photon flux, amount basis);
- $A(\lambda)$ is the absorbance at the excitation wavelenght.

The most reliable method for recording ΦF is the comparative method of Williams *et al.*[104], which involves the use of well characterised standard samples with known ΦF values. Essentially, solutions of the standard and test samples with identical absorbance at the same excitation wavelength can be assumed to be absorbing the same number of photons. Hence, a simple ratio of the integrated fluorescence intensities of the two solutions (recorded under identical conditions) will yield the ratio of the quantum yield values. Since ΦF for the standard sample is known, it is trivial to calculate the ΦF for the test sample.

The lifetime is also important. The lifetime of a fluorophore is the average time between its excitation and return to the ground state. It determines the time available for the fluorophore to interact with or difuse in its environment, and hence the information available from its emission. It is given by:

$$F(t) = F_0 e^{-t/\tau} \qquad (2)$$

The emission rates of fluorescence are tipically 10^8 s^{-1}, so that a typical fluorescence lifetime is near 10 ns.

1.5.3. Fundaments of the Technique

Fluorescence is based on the property of some molecules that when they are hit by a photon, they can absorb the energy of that photon to get into an excited state. Upon relaxation from that excited state, the same molecule releases a photon: fluorescence emission. The energy difference between the absorbed and emitted photons ends up as molecular rotations, vibrations or heat. Sometimes the absorbed photon is in the ultraviolet range, and the emitted light is in the visible range, but this depends on the absorbance curve and Stokes shift of the particular fluorophore.

Once a molecule has adsorbed energy in the form of electromagnetic radiation, there are a number of routes by which it can return to the ground state. The following graphic, termed a Jablonski diagram, shows a few of these processes.

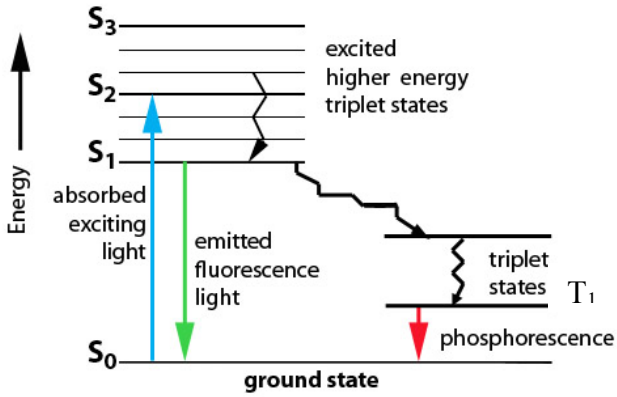

Figure 10. Jablonski diagram (source: http://web.uvic.ca/ail/techniques/Jablonski.jpg).

If the photon emission occurs between states of the same spin state (e.g. S_1 --> S_0) this is termed fluorescence. If the spin state of the initial and final energy levels are different (e.g. T_1 --> S_0), the emission is called phosphorescence. Since fluorescence is statistically much more likely than phosphorescence, the lifetimes of fluorescent states are very short and phosphorescence somewhat longer, sometimes even hours).

The energy of the photon that is released is always lower than that of the photon that was absorbed. So the photon that excites the dye always has a smaller wavelength than the photon that gets emitted (Stokes Shift).

Generally fluorescence is used as a non-destructive way of tracking or analysis biological molecules. Some protein or small molecules in cells are naturally fluorescent; this is called intrinsic fluorescence or autofluorescence. Instead, some proteins, nucleic acids or other small molecules can be "labelled" with an extrinsic fluorophore.

Dyes don't get excited by just one exact wavelength, but by a range of wavelengths around a peak, the excitation spectrum. When people talk about the excitation wavelength of a dye, they usually mean the peak of the excitation spectrum. The same is true for emission; there is an emission spectrum, characterized by a peak in the spectrum.

There are however some drawbacks associated with the techniques. Dye sensors distributed in the cell matrix are sometimes hard to calibrate due to matrix effects such as uneven dye distribution and highly unpredictable quenching conditions. Further, there are severe problems with signal drift due to photobleaching even though fluorescence is normalized by quotients[105]. To minimize these effects, calibrations before and after the experiment (i.e. time correlated calibrations), facilitate compensations for signal drift over time and help keeping track of analytical performance during the experiment[106,107]. Due to this procedure, dye interactions are minimized and the accuracy of the measurements is maintained.

1.5.4. Spectrofluorometers

The spectrofluorometer is an instrument which takes advantage of fluorescent properties of some compounds in order to provide information regarding their concentration and chemical environment in a sample. A certain excitation wavelength is selected, and the emission is observed either at a single wavelength or a scan is performed to record the intensity versus wavelength also called an emission spectra.

Generally spectrofluorometers use high intensity light sources to bombard a sample with as many photons as possible. This allows for the maximum number of molecules to be in the excited state at any one point in time. The light is either passed

through a filter, selecting a fixed wavelength, or monocromator, which allows to select a wavelength of interest to use as the exciting light. The emission too is either passed through a filter or a monochromator before being detected by a PMT, photodiode, or a CCD detector. The signal can either be processed as a digital or analog output. Systems vary greatly and a few things must be considered when choosing. First is signal to noise, sensitivity and detection limit. These systems come with many options including:

- Polarizers;
- Peltier temperature controllers;
- Cryostats;
- Cold Finger Dewars;
- Pulsed Lasers for lifetime measurements;
- LEDs for lifetimes;
- Filter holders;
- Adjustable optics (very important);
- Solid sample holders;
- Slide holders;
- Integrating spheres;
- NIR detectors;
- Bilateral, manual and computer controlled slits;
- Fast switching monochromators;
- Filter wheels;

1.5.5. Ratiometric Measurements

Absolute fluorescence intensity is notoriously hard to standardize, because it is directly dependent on dye concentration and instrumental factors such as lamp intensity and detection efficiency[108]. Dye concentration decreases continually due to bleaching and leakage, effects that can be minimized but not completely eliminated. Yet, the above uncertainties are substantially cancelled by performing ratiometric measurements. For doing so is necessary to have instrumentation that allows rapid alternation between multiple excitation wavelengths.

Ratio imaging of fluorescent indicators is an extremely powerful tool for studying dynamic intracellular biochemistry in multiple individual cells. The same principle of ratio imaging can also be used to quantify the distribution of specific proteins, to map the concentration of different messengers and to map interactions between molecules[109]. Normalization procedures based on fluorescence intensity ratios have increased the analytical performance of these measurements dramatically[105] and are nowadays fairly applicable for quantification.

1.5.6. pH Measurements

Extra and intracellular qualitative measurements of ions using fluorescent dyes have been used successfully over the past 30 years[110]. It is now consensual that pH plays important roles in many cellular activities[111]. A variety of techniques have been described which measure cellular pH, each having advantages and limitations[112]. The two most specific methods are micro pH electrodes and fluorescent pH indicators[113,114].

Small molecule fluorophores can be used to measure pH and ion concentrations[115]. Fluorescence pH-indicators may be used for either acid base titrations or for indicating the actual pH-value of a solution. The application of these pH-sensitive fluorescent probes represents both a progressive and easy way of in-vivo determination of pH values.

Unfortunately, it is not always possible to select an analytical wavelength which is absorbed by just one of the differently charged species. For most indicators the choice of the excitation wavelength is of high significance with respect to the resulting titration

curve. To find an ideal indicator for making precise pH measurements in the near neutral range the following properties have to be considered:

- A pKa-value in the 6 to 8 range, ideally 7.4;

- High fluorescence quantum yield;

- High molar absorptivity in order to make optimal use of incident light;

- The excitation maximum should lie in the visible part of the spectrum to allow use of lamps rather than the more expensive UV-light sources. Also, fiber optics for visible light are cheaper than those for UV-light;

- Good water solubility;

- Fluorescence should not be influenced (e.g. quenched) by other molecules in solution;

- Photostability;

- A large Stokes' shift between excitation and emission maximum. This allows the use of commercially available glass filters without filtering off parts of the incident or emitted light.

Protons can therefore be detectable by pH-sensitive indicators, particularly HPTS. Its pKa is optimal near typical cytosolic pH, its leakage rate is relatively slow, and it has a pair of excitation wavelengths suitable for comparison by ratio. So the ratio obtained from the two wavelengths indicates pH while cancelling fluctuations.

1.5.7. Single-Cell Measurements

The high-throughput automated fluorescence imaging of biological processes in living cells is currently technically challenging, and requires robust and simple

fluorescent labelling techniques. The fluorescent reporters need to be specific, they must interfere as little as possible with the biological process being visualized and they must not perturb the global physiological conditions of the cells. Most importantly, the labelling and detection procedures have to be quantitative and highly reproducible so that different experiments that have been carried out at different times can be compared, and so that image data can be evaluated using an automated phenotypic analysis[116].

The ability to measure fluorescence using single cells expands considerably the range of tissue types and biological problems that can be adressed. Only a few good cells are needed to keep one busy for an experimental day. Particularly interesting subsets of cells can be picked out and their metabolites measured with little or no interference from their neighbors or dead cells. Cell morphology can be directly compared. Leaked dye and absorbing or fluorescing additives in the medium cause much less significant artifacts than they do in larger scale because illumination and observation are focused on the cells of interest while the intercellular space is mostly masked off.

Observations on single molecules represent the highest obtainable sensitivity and they have already been performed in some laboratories[117]

1.5.8. Fluorophores

A fluorophore is, in analogy to a cromophore, the part of a molecule which makes it to be fluorescent. It is a functional group that will absorb energy of a specific wavelength and re-emit it at a lower (but equally specific) wavelength (fig. 11). Both amount and wavelength of the emitted energy depend on the fluorophore and on its chemical environment. The fluorophore can be a protein, a quantum dot or a small molecule.

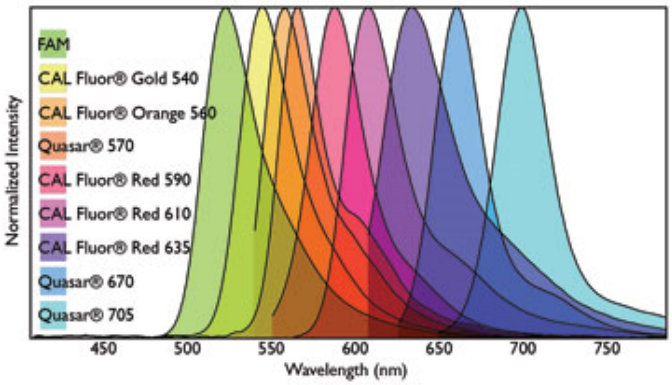

Figure 11. Normalized emission spectra for a series of fluorophores (source: www.biosearchtech.com/.../multiplexing-qpcr)

The fluorescent properties of a fluorophore are determined by its chemical structure. When a fluorophore is dissolved, the solvent, usually a salt solution, will affect the fluorophores chemical surroundings. This can affect its chemical structure which in turn changes its fluorescent properties. This is the basis for using dyes as sensors.

The dye will bind the ion to measure and the binding of the ion induces a structural change that changes the dyes fluorescent properties. It can do this in two ways: by increasing the quantum efficiency of the dye, making it brighter; or by changing the spectral characteristics of the dye, shifting the wavelengths at which the dye gets excited or at what wavelengths it emits. When only the brightness changes, it is a so called "single excitation – single emission dye". When the wavelength at which the dye is excited changes, it is usually refered to as a dual excitation dye.

All fluorophores are aromatic or conjugated since they fluoresce thanks to delocalized electrons which can jump a band and stabilize the energy absorbed. When the dye contains an electron-donating and an electron-accepting group at opposite ends of the aromatic system, this dye will probably be sensitive to the environments polarity (solvatochromic), hence called environment-sensitive. This characteristic makes certain fluorophores to be excellent sensors/indicators.

Fluorophores provide good spatial and temporal resolution[118,119], they can be used with motile cells[118] and can be applied to cell populations[120].

1.5.8.1. HPTS

8-Hydroxypyrene-1,3,6-Trisulfonic Acid (HPTS, also known as pyranine H348) is an inexpensive, highly water soluble, membrane impermeant pH indicator with a pKa of ~7.3 in aqueous buffer[121]. The pKa is reported to rise to 7.5-7.8 in the cytosol of some cells[122]. HPTS exhibits a pH-dependent absorption shift, allowing ratiometric measurement susing an excitation ratio of 450/405 nm[123].

Tanasugarn laboratory has long used HPTS fluorescence excitation method to measure pH in single, living cells[111,118,124] "cellular map" of cytoplasmic pH based on the HPTS fluorescence excitation ratio method..

HPTS shows a strong absorption band at around 450 nm in alkaline solution, its fluorescence increases with pH and disappears when the solution becomes acidic. Only the phenolate (base form) is able to absorb light, when excited at 450 to 490 nm. The more acidic the solution becomes, the less light will be absorbed and consequently also emitted. Under these conditions continuous changes in fluorescence intensity are observed. The reverse can be true when exciting at another wavelength, in the case of HPTS at 405 nm. A fluorescence signal may become even pH invariable when excitation is done at the isosbestic wavelength of the excitation spectrum (at 415 nm for HPTS)[121].

Due to its unusual stability in the pH 0-14 range, and its other favourable properties, HPTS is considered to be the most suitable fluorescence indicator for both pH measurements in the near neutral range, and for titrations. Its triple or quadruple negative charge (Fig. 12) should render it membrane-impermeable, which would allow the measurement of extracellular pH-values and pH-changes. Finally, functions other than the hydroxy group in the molecule offer a possibility for the immobilisation of the indicator on a polymeric support[121].

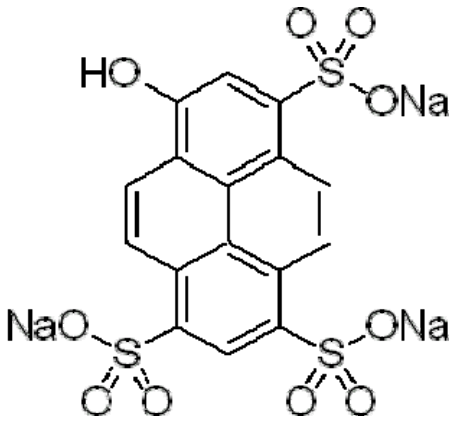

Figure 12: HPTS.

The unique pH-dependent spectral properties, high water solubility, high fluorescence quantum yields, visible excitation and emission, large Stokes' shift and low cost of HPTS make its applications numerous. They include:

- Detecting proton permeability in lipossomes and cells[125,126];

- Investigating pH-mediated changes of intracellular Ca^{2+}[127];

- Fiber-optic sensing of oxygen and carbon dioxide[128] and enzymatic activity[129];

- Detecting bioenergetically linked proton-transfer processes[130,131];

- Measuring acidity of lysosomes and other organelles[132];

- Detecting membrane fusion and lysis[133];

- Following endocytosis[134];

- Detecting targeted intracellular delivery of liposome-encapsulated molecules[135,136];

- Measurement of red cell volume changes[137];

- As a sensitizer[138];

- Other purposes[139]

Its toxicity is very low[140]. Wolfbeis group has found that it may be purified by fractionated crystallization from methanol[121]. They also demonstrated that the signal change as a function of the pH-value may become reversed[121]; when excited at 405 nm, light absorption increases when the solution goes acidic, thereby leading to an increase in fluorescence intensity with decreasing pH. So, by proper selection of the excitation wavelength pH-changes may be followed by an increase or by a decrease of fluorescence intensity.

When excited at the isosbestic wavelength of excitation, fluorescence intensity is pH-invariable. It should be borne in mind that HPTS always fluoresces from its anionic form in the pH 0-14 range as a result of photodissociation in the first excited singlet state.

The pKa-value of HPTS is dependent upon the nature and the ionic strength of the solution (Table 1). At physiological ionic strengths it is in the favourable 7.3 range[121].

Table 1. Photometrically determined pKa, values of HPTS at 22ºC in various kinds of solvents[121].

Solution	pKa-Value
Pure water	8.04 ± 0.07
Water with 0.0066 M phosphate buffer	7.51 ± 0.03
Water with 0.066 M phosphate buffer	7.29 ± 0.02
Water with 6 % albumin	7.83 ± 0.06
Water with cetyl trimethylammonium bromide (Cationic surfactant, conc. 6.6mM)	7.69 ± 0.03
Water with sodium dodecylsulphate (Anionic surfactant, conc. 50 mM)	7.43 ± 0.06

Fluorescence quantum yields are almost 100 % in both alkaline and acidic solution when excited with light of 2 higher than 400nm. When excited by UV light they seem to be somewhat lower. Fluorescence decay times of HPTS are invariably 5.3 ns in the pH 2-13 range. After addition of water the blue fluorescence decreases in favour of the green anion fluorescence[121].

1.6. MALDI-TOF-MS – An Overview

Until recently MS could not be used for analysis of larger molecules such as proteins and nucleic acids, since these were broken down during the ionization process. Soft ionization methods such as MALDI (Matrix assisted laser desorption and ionization) now make it possible to analyze larger molecules without fragmentation[141] (proteins, peptides, sugars, polymers and other macromolecules, which tend to be fragile and fragment when ionized by more conventional ionization methods). MALDI is also the method of choice for recording intact protein distributions. MALDI can analyze hundreds of proteins directly from tissue sections[142]. It is particularly effective in protein analysis, allowing the determination of molecular weights with accuracy of the order of 1/1000 and a mass range up to 10^6 Da. The analysis of cell systems is also very common achieving, likewise , very low mass detection limits[143].

Because of some inherent advantages of the MALDI process, such as relatively low sample requirements, sensitivity and extended lifetime of the sample on the target plate, the coupling of MALDI to nearly every mass spectrometer available has been either exemplified or is already in use and commercially available[144]. The type of a mass spectrometer most widely used with MALDI is the TOF (time-of-flight).

MALDI-TOF was introduced in 1987-1988 by two different groups[143,145] and for many nonexperts has become a linked synonym[144].

MALDI-TOF/TOF high-resolution tandem mass spectrometer (Figure 13) combines the advantages of high sensitivity and accuracy, advanced software capabilities for peptide analysis associated with MALDI and comprehensive fragmentation information provided by high-energy collision-induced dissociation (CID), which is mediated by the use of collision neutral atoms or molecules in the gas phase like He, Ar, air or Xe, and subsequent dissociation of the ion[146,147].

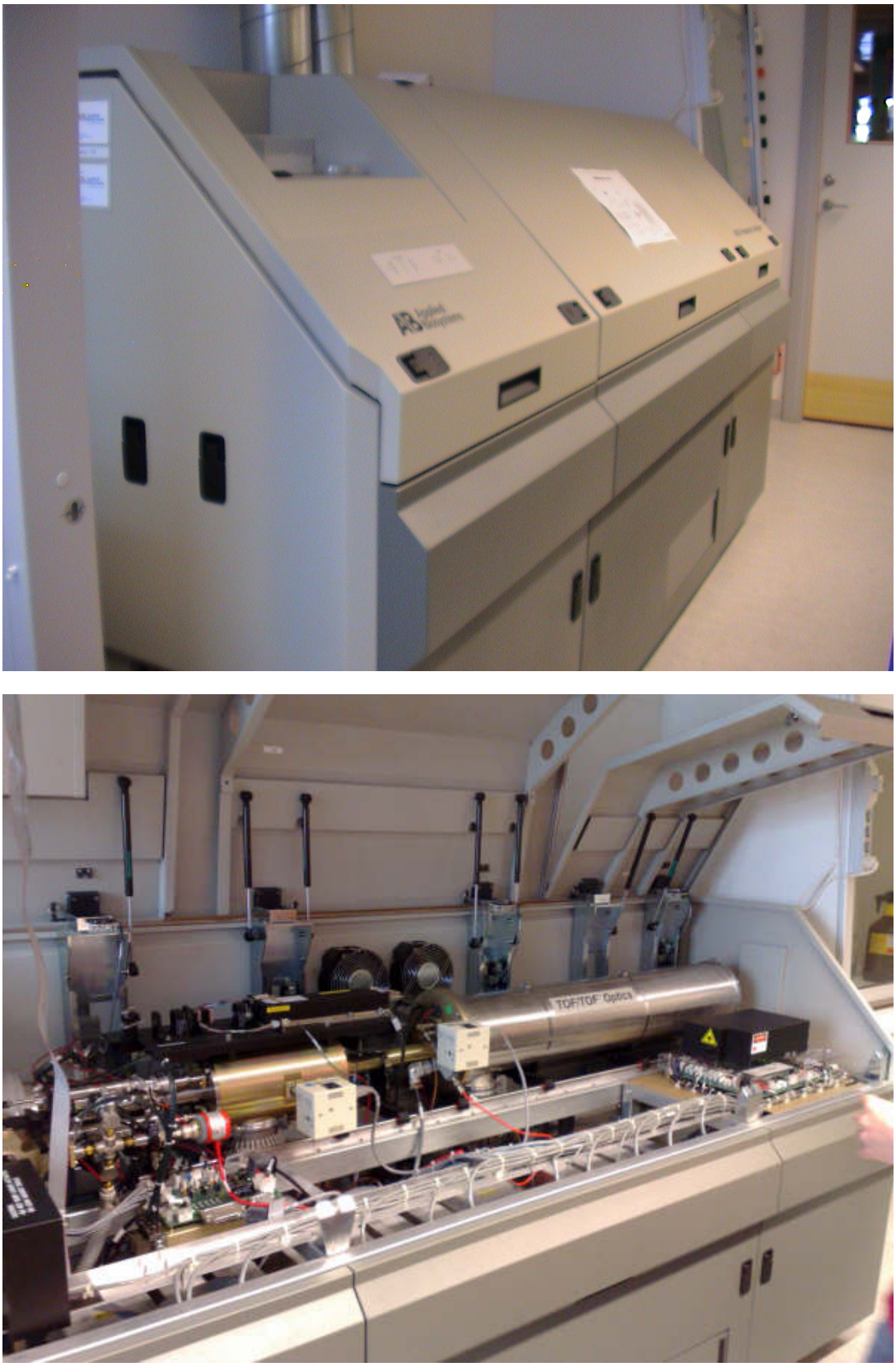

Figure 13. Close up of a 4700 MALDI-TOF-TOF instrument from Applied Biosystems; from the outside (up) and the inside (down).

1.6.1. Fundaments of the Technique

MALDI is a complex chemical event (one-laser-shot-one-mass-spectrum); it is, moreover, happening within the time scale of a few nanoseconds[144]. Despite the involvement of a very low absolute amount of material, a dense plume of material containing matrix neutrals as well as reactive species, such as matrix radicals, electrons, hydrogen atoms[148] is formed which is expanding into the vacuum of the mass spectrometer ion source.

In MALDI, analytes are mixed in a flat metal plate with a light-absorbing matrix compound. During evaporation, matrix and analyte co-crystallize in a MALDI spot. Laser desorption of these matrix crystals entrains the large molecules to bring them into the gasphase[149]. Gas-phase chemistry between the matrix and analyte molecules can ionize a large fraction of the entrained analyte molecules[150]. The ions created in the desorption event are extracted and accelerated against the detector through a potential difference applied in front of the target. The ions then fly at a constant velocity and are separated through field-free vacuum, according to their mass-to-charge ratios. The ions then hit the detector at the end of the tube and a computer is used to register the flight time which can be converted to an m/z spectrum (heavier particles reach lower speeds).

MALDI-TOF instruments are typically equipped with an "ion mirror", deflecting ions with an electric field, thereby doubling the ion flight path and increasing the resolution (Figure 14).

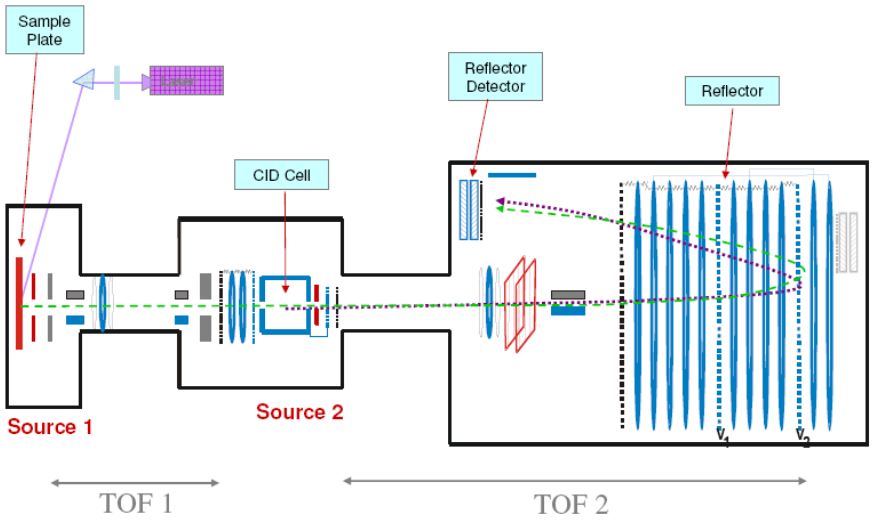

Figure 14. Schematic of a 4700 MALDI-TOF-TOF instrument from Applied Biosystems.

1.6.2. Matrix Properties and Sample Preparation

The sample preparation in MALDI is crucial for the result. The choice of matrix solution, matrix composition, size of matrix crystals, the method of matrix application, the addition of TFA and formic acid, delay between laser pulses, delay time of the acceleration power, laser wavelength, energy density of the laser and the impact angle of the laser on the target are among others the critical values for the quality and reproducibility of the method.

Matrixes are aromatic weak acids which strongly absorb energy at the wavelength of the laser beam.

The choice of matrix is fundamental to the success of the technique being detrimental to sensitivity[151]. It is responsible for extracting the molecules from the sample, its vaporization and ionization at the same time that prevents the aggregation of analyte molecules and protects the biomolecule from being destroyed by the laser beam[152,153]. Besides, formation of analyte-doped matrix crystals segregates the analytes from detrimental co-factors such as salts[154].

The matrix substance is often dissolved in an organic solvent (normally acetonitrile or ethanol) mixed with highly purified water. Trifluoroacetic acid (TFA) may also be added. The organic solvent allows hydrophobic molecules to dissolve into the solution, while the water allows for water-soluble (hydrophilic) molecules to do the same. The analyte is mixed with the matrix in a large molar excess compared to the analyte (usually on a ratio in the range of 1:100 up to 1:50000 depending on what is optimal for ion production and avoidance of suppression effects).

The three most commonly substances used as matrix are 3,5-dimethoxy-4-hydroxycinnamic acid or sinapinic acid (SA), α-cyano-4-hydroxycinnamic acid (CHCA) and 2,5-dihydroxybenzoic acid (DHB).

General recommendations of matrices for each molecular class have been summarized[155]. It has been reported that SA provides the best signals for higher molecular weight proteins, whereas CHCA is more suitable for lower molecular weight peptides[156].

1.6.3. Real-Time Sampling for MS Detection

Over the years, efforts to understand electrospray ionization (ESI) have led to detailed examinations of the behavior of neutral and charged droplets subjected to external electric fields. For example, Gomez & Tang observed fissioning of charged droplets to form much smaller progeny droplets to be an important component of the ESI-MS process[157]. As these progeny droplets can be sampled by MS, this phenomenon can be exploited as a means of probing the contents of levitated droplets non-destructively.

Grimm & Beauchamp demonstrated controlled extraction of droplet streams from larger droplets passing through an electric field of *ca.* 2×10^6 V/m; the droplet streams were ionized and could be sampled with MS[158,159]. In preliminary experiments carried out in our group, Tabaei achieved a similar result with levitated droplets enclosed by ring electrodes[160]. Droplet "spitting" was observed.

Another approach towards MS interrogration of levitated droplets, developed by Westphall *et al.* in the group of Lloyd Smith, involves controlled charging of the droplet with a corona discharge, followed by laser desorption of ionized material which is sampled into the MS entrance orifice[161]. The advantage of such an approach is that extraction of ions into the MS can be done with much lower applied voltages. The need for a high concentration of an acidic matrix – as in MALDI with UV lasers – makes this variant of the method unsuitable for experiments designed to deal with living cells.

Along these lines, Rapp *et al.* have used short, 2 mJ pulses of 2.9 μm IR to nebulize liquid and droplet streams (*e.g.* not levitated), producing ions which could be analyzed with high sensitivity by MS[162]. A new approach would involve desorbing neutral material from a levitated droplet with an IR laser pulse, followed by postionization with the plume of an electrospray ionization source. Such a scheme was demonstrated by Shiea *et al.*[163].

2. Matherial and Methods

2.1 The Airborne System

The instrumental set-up is shown in figure 15:

Figure 15. Instrumental set-up.

An 100 kHz ultrasonic levitator APOS BA 10 (DANTEC/invent Measurement Technology GmbH, Erlangen, Germany) was used for contactless sample handling in the sub micro liter volume range.

The levitator generates a standing wave with equally spaced nodes and antinodes by multiple reflections between an ultrasonic radiator and a solid reflector. The liquid droplets are then levitated in the nodal points of the standing ultrasonic wave. Since the levitated sample is maintained at a fixed position at any time interval, it is not disturbed by contact of any other surface than the surrounding medium – air.

The technique utilizes an in-house developed piezoelectric flow-through droplet dispenser for precise reagent supply. The dispenser was developed in-house using silicon micromachining methods. The dispensed droplets are ejected from a flow-trough channel formed by joining two microstructered silicon plates, 13 mm long, 6mm wide and 250 µm thick each. The flow-through channel measures 8 mm x 1 mm x 50 µm,

having a volume of 400 nL. In the center of the channel, a protruding pyramid shaped nozzle in the centre of the channel of 40×40 μm size is formed. By applying a short voltage pulse across a multilayer piezoelectric element connected to a push-bar in the channel wall opposite the nozzle. It elongates and pushes into to the channel generating a pressure pulse in the liquid. The increased pressure accelerates the liquid in the nozzle and a droplet is ejected. The volume of the ejected droplets is dependent on the size of the dispenser nozzle, the shape of the voltage pulse and liquid parameters like surface tension, viscosity and density.

The dispenser was mounted on XYZ-micropositioning stages throughout the experiments in order to facilitate alignment. This device is capable of ejecting droplets at a rate of up to 500 Hz by pulsing the piezo-electric element [69,78,82].

During the levitation experiments, the dispenser for water and reagent addition was set to eject 65 picoliter droplets at a rate of 10 Hz with a pulse length of 10 μs and a burst frequency of 30 Hz. This was done continuously when the aim was to compensate for evaporation. A pre-determined number of droplets were set, for reagent addition to a chosen concentration.

For excitation of the droplet fluorophore HPTS, a PIT® with a L-201M illumination subsystem was used, which is comprised of a compact arc lamp housing coupled to a model 101 computer controlled monochromator. This assembly is coupled to a microscope via a fiber optic cable. The monochromator includes a shutter. Illumination can be generated from 200 to 1000 nm. Continuously variable micrometer-adjusted slits provide bandpass control. The bandpass is 4 nm/mm and is used with the standard 1200 lines/mm grating. The sample handling subsystem is a MP-1 sample compartment designed to accept up to two excitation and two emission subsystems. It is easily configured for L- or T- format. The system uses high grade quartz lenses to focus the excitation beam on the sample and to collect emmited light. It features filter holders on all ports, and mechanical lid-activated shutters on the emission ports. The detection system is the model 814 analog/photon-counting photomultiplier detectot, which is a compact unit that is fitted to a model 101 monochromator.

The lamp power supply, PTI LPS-220B, is a high-regulated DC power supply that provides very stable power for xenon, mercury and mercury/xenon compact arc lamps.

2.2. Evaporation Rate and Volume control

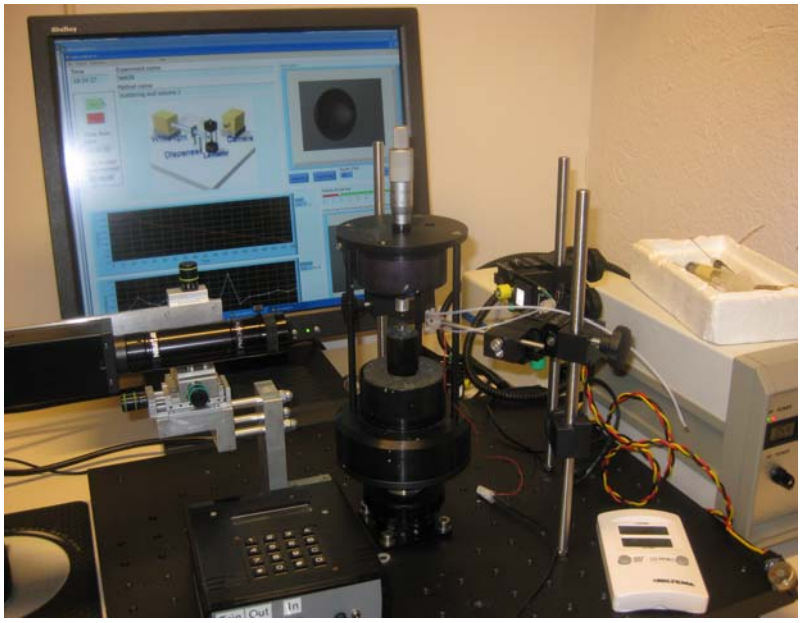

Figure 16. Set-up for volume measurements.

The basic idea for the volume calculation is to record pictures of the droplet through time and determine the droplet diameter. The droplet volume can then be estimated by assuming rotational symmetry around the z-axis. This can be done automatically by using an appropriated imaging system and software (Fig.2). A microscope connected to a CCD camera, mounted on XYZ-micropositioning stages, was used for droplet imaging. Both volume and light scattering can be registered on-line by a computer connected to the CCD camera. Afterwards, in order to compensate for evaporation, the proper rate for water to be added to the droplet with the help of the dispenser can be estimated.

2.3. pH Measurements

Detection of pH changes in the acoustically levitated droplet are followed using the pH-dependent fluorophore HPTS and fluorescence imaging detection.

FFAs are released during the lipolysis, which in turn results in a pH-decrease in the extracellular buffer. A proton is released for each free fatty acid with the concommitent pH decrease of the surrounding buffer droplet. By using the titration buffer with low buffering capacity and the pH dependent fluorophore HPTS, the pH decrease in the levitated droplet can be monitored. This pH-indicator, with a pK_a of ~7.3 in aqueous buffers, exhibits a pH-dependent absorption shift and has an emission maximum at 510 nm. The fluorescence intensity of HPTS increases when exciting at 455 nm and decreases at 405 nm with decreased pH.

Sample droplets of 1μL containing the desired number of adipocytes and the pH-sensitive fluorophore (10 μM) are levitated in the ultrasonic levitator. The lipolysis is inhibited with insulin; either added with the flow-through dispenser (human insulin) or secreted in-droplet by mouse pancreatic β-cells. The reagent additions are tuned to give the desired concentration in the levitated droplet. Water is added at a rate chosen to counter-balance droplet evaporation.

2.4 MALDI-TOF

Samples were analysed using MALDI-TOF MS. A semi-saturated solution of α-4-hydroxycinnamic acid (CHCA), in 50% of acetonitrile, 0,1% of TFA and 0,1M of citric acid, was used as the MALDI matrix for all analysis, except for the adipocyte samples. Solutions of Sinapinic acid (SA) and 2,5-dihydroxybenzoic acid (DHB), using acetonitrile and trifluoroacetic acid in variable concentrations were used for analysis on the adipocytes. Mass spectrometric measurements were performed on a 4700 proteomics analyser MALDI TOF/TOF instrument (Applied Biosystems®, Framingham, MA,USA).

The presented spectra are the sums of 5000 single-shot spectra. Mass spectra were acquired in the linear mode using delayed ion extraction. All the other features were variable.

2.5. Glycation process by dynamic dialysis method

20 mL of 1.0 mg/ml human insulin solution was placed in dialysis bag (cut off 3.0 kDa) and put in a dialysis jar filled with 200 ml of 1.6 M D(+)-glucose-monohydrate dissolved in 100mM phosphate-buffer saline (pH 7.4) at 37 ºC for sixteen days. The glucose solution was changed every day. After the glycation process was terminated, Centricon Centrifugal Filter Devices, Centricon YM-3 (Millipore, Bredford, MA, USA) were employed to remove low molecular weight compounds. The products of glycation were assayed by MALDI-TOF.

2.6. Fluorophore test – acetic acid (HAc) titration

A 1 μL droplet containing titration buffer (131 mM NaCl, 4.74 mM KCl, 2.54 mM $CaCl_2$, 1.19 mM KH_2PO_4, 1.19 mM $MgSO_4$, 1% (w/v) BSA, 2 mM glucose, 200 nM adenosine) and 10 μM HPTS in 1 mM PBS (pH 7.4), was suspended in the nodal points of the standing wave in the acoustic levitator. A continuous addition of 10 mM acetic acid (HAc) to the levitated droplet was done by the micro flow-through dispenser, at a frequency of 10 Hz. The fluorescence was measured using excitation wavelengths of 405 and 455 nm. The emission was registered at 510 nm.

2.7 β-cells

Individual β-cells from mouse pancreatic islets were supplied by the Department of Clinical Sciences in Malmö, Unit of Islet Cell Exocytosis, Lund University Diabetes Centre, Clinical Research Centre, Malmö. The β-cells were prepared from pancreatic Langerhans islets following incubation incubation and vigorous shaking in calcium-free solution. The medium was then exchanged for RPMI 1640 with Heppes Buffer. Before experiments, the medium was exchanged for the titration buffer described above for adipocytes.

2.8. Adipocytes

Adipocytes were provided by the Department of Experimental Medical Science, Division for Diabetes, Metabolism and Endocrinology, Biomedical Center, Lund University, Lund. Adipocytes were isolated from male Sprague-Dawley rats by collagenase digestion[164,165]. The cells were kept in a Krebs-Ringer-HEPES buffer (*storage buffer*) pH 7.40 (118.6 mM NaCl, 4.74 mM KCl, 2.54 mM $CaCl_2$, 1.19 mM KH_2PO_4, 1.19 mM $MgSO_4$, 25 mM HEPES) containing 1% (w/v) bovine serum albumin (BSA), 2 mM glucose and 200 nM adenosine. Every two hours, the storage buffer was removed and the cells were washed with new storage buffer. Before experiments, the storage buffer was exchanged for a *titration buffer* with pH 7.40 and low buffering capacity (131 mM NaCl, 4.74 mM KCl, 2.54 mM $CaCl_2$, 1.19 mM KH_2PO_4, 1.19 mM $MgSO_4$) containing 1% (w/v) BSA, and 200 nM adenosine. The titration buffer also contained 100 nM hydroxypyrene-1,3,6-trisulfonic acid (HPTS) and different concentrations of glucose (5 or 15 mM).

2.9. Reagents

Human insulin was a gift from Novo Nordisk®, Gentofte, Denmark. For the experiments with adipocytes, a stock solution of 0.25 μM was prepared in water to give a concentration in the levitated droplet of 1 nM. Acetylcholine chloride was obtained from Sigma-Aldrich®, Sweden. A stock solution in water of 8 M was prepared to obtain a concentration after addition to the levitated droplet of ~350 μM. (-)-Isoproterenol(+)-bitartrate salt (Isoprenaline) was obtained from Sigma-Aldrich® (St. Louis, MO, USA). A stock solution of 25 μM was prepared to give a concentration of 100 nM after addition to the levitated droplet. Sinapinic acid and α-cyano-4-hydroxy cinammic acid were obtained from Sigma-Aldrich®, Sweden..

The water used in all solutions was prepared using a Milli-Q system (Millipore, Bedford®, MA, USA).

The pH dependent fluorophore was the trisodium salt of hydroxypyrene-1,3,6-trisulfonic acid (HPTS) from Molecular Probes (Eugene, OR, USA). This fluorophore has a pKa of ~7.4 in aqueous buffers and is ideal for measurements in the near neutral

pH-range. It exhibits an emission maximum at 511 nm and allows for ratiometric measurements using an excitation ratio of 455/405 nm.

2.10. General Considerations

All the samples were collected with a micro syringe and placed on the nodal points of the acoustic levitator with the help of a capillary. The droplet is then removed from the tip of the syringe by a fused-silica capillary that is then deposited in the ultrasonic field. The droplet was not drawn in by the capillary, only allowed to hang from the tip. With optimal settings the droplet is spherical. After each experiment, cell number in the levitated droplet was determined by counting the cells using a microscope. Some of the droplets were, however, collected onto a MALDI plate, coated with the matrix and left to dry, for ensuing analysis.

Adipocytes are subject to floatation, having lower density than the surrounding aqueous buffer, so it is important to maintain a slight mixing in the levitated droplet. Streaming effects inside the droplet and/or on the droplet surface[166], lead to a slight mixing of the sample. A more efficient mixing, however, is achieved by slightly distorting the standing wave by adjusting the distance between the ultrasonic transducer and the reflector. A synthetic β-adrenergic agonist (isoprenaline) is added to stimulate adipocyte lipolysis whilst insulin is added inhibiting it.

The reagent additions with the dispenser are tuned to give the desired concentration in the levitated droplet. Initially all the droplets have 1 μL volume.

3. Results and Discussion

3.1. Emission and Excitation Spectra of HPTS

Both emission and excitation wavelenghts of HPTS were estimated and its pH dependence studied using a variety of pH buffers. Two main excitation wavelenghts were found at 405 and 455 nm (Fig. 17) while a single, well defined emission peak rises at 510 nm (Fig. 18). An isosbestic point was found at 415 nm (Fig. 17).

The fluorescence of HPTS decreases with pH when exciting at 405 nm. The reverse is true when exciting at 455 nm. A fluorescence signal may even become pH invariable when excitation is done at the isosbestic wavelength of the excitation spectrum (in the given case at 415 nm).

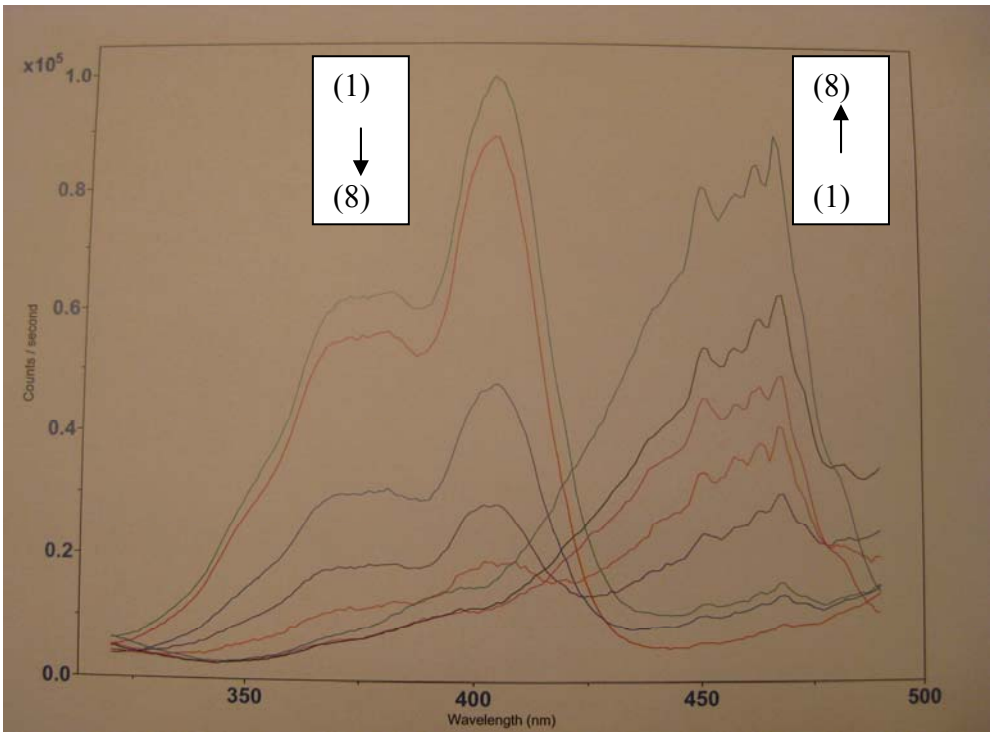

Figure 17. Excitation spectra of 1 μM HPTS in various pH citrate buffers (1) 3.00; (2) 4.00; (3) 5.00; and phosphate buffers (4) 6.00; (5) 7.00; (6) 8.00; (7) 9.00; (8) 10.00. Emission wavelenght at 510 nm.

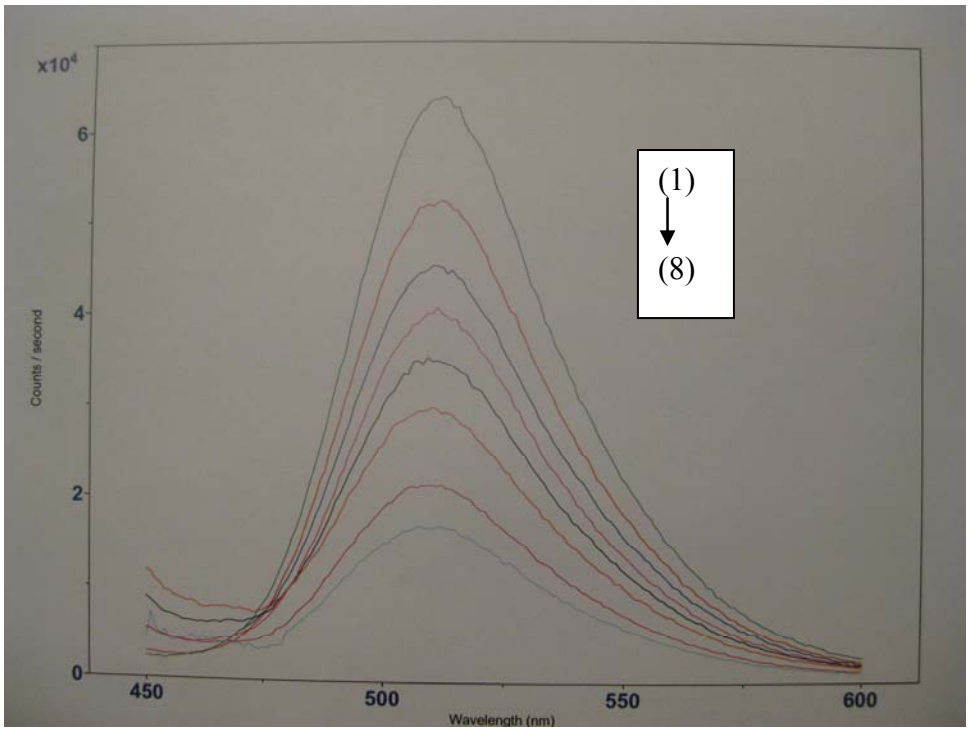

Figure 18. Emission spectra of 1 μM HPTS in various pH citrate buffers (1) 3.00; (2) 4.00; (3) 5.00; and phosphate buffers (4) 6.00; (5) 7.00; (6) 8.00; (7) 9.00; (8) 10.00. Excitation wavelenght at 405 nm.

3.2. Acetic Acid Titration

In figure 19 we can see the dependence of fluorescence intensity on concentration. By simply leaving a droplet to evaporate both emission intensities when exciting at 405 and 455 nm increase. This is due to the concentration effect.

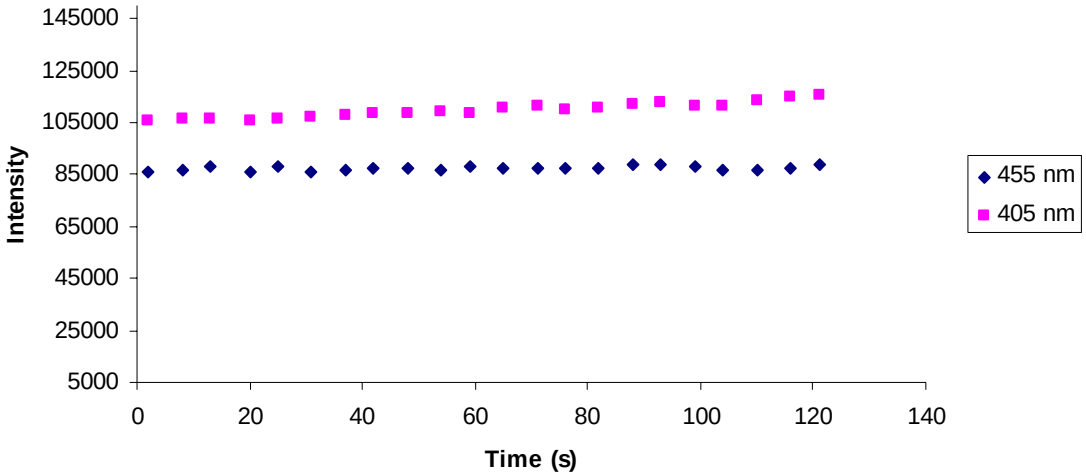

Figure 19. Effect of droplet evaporation and concomitant increase in concentration.

A 1 µL buffer droplet containing the fluorophore (HPTS, 10 µM) was excited alternatedely at 405 and 455 nm and its correspondent intensity (I_{405}, I_{455}) measured at the maximum emission wavelength, 510 nm. Shooting continuously a solution of acetic acid (HAc), 10 mM at a frequency of 10 Hz led to a decrease of the pH in the droplet (fig. 20). As expected, the fluorescence intensity corresponding to the excitation at 405 nm increased whilst the opposite happened when exciting at 455 nm.

The ratio I_{405}/I_{455}, varies in accordance to pH (fig. 21). Therefore, given that it is possible to calculate the concentration in HAc through time, the pH of cell-containing droplets can be easily estimated. As the pH goes down, the intensity ratio gets closer to a minimum, almost not decreasing despite continuous addition of the acid. This means that the minimum for the interval of the fluorophore response has been reached.

Because the ratio between the pair of wavelengths is used the fluorescence variations due to uneven dye content are normalized.

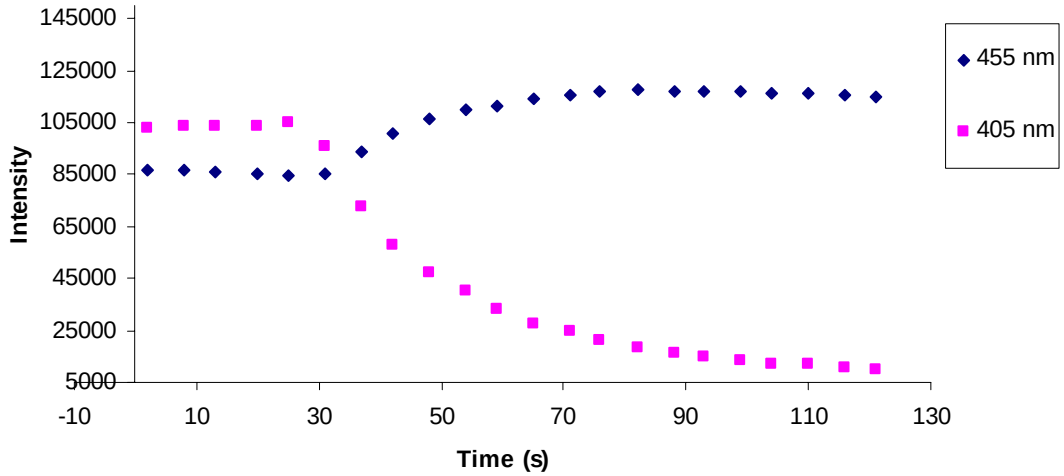

Figure 20. Titration of a buffer droplet with acetic acid, 10 µM.

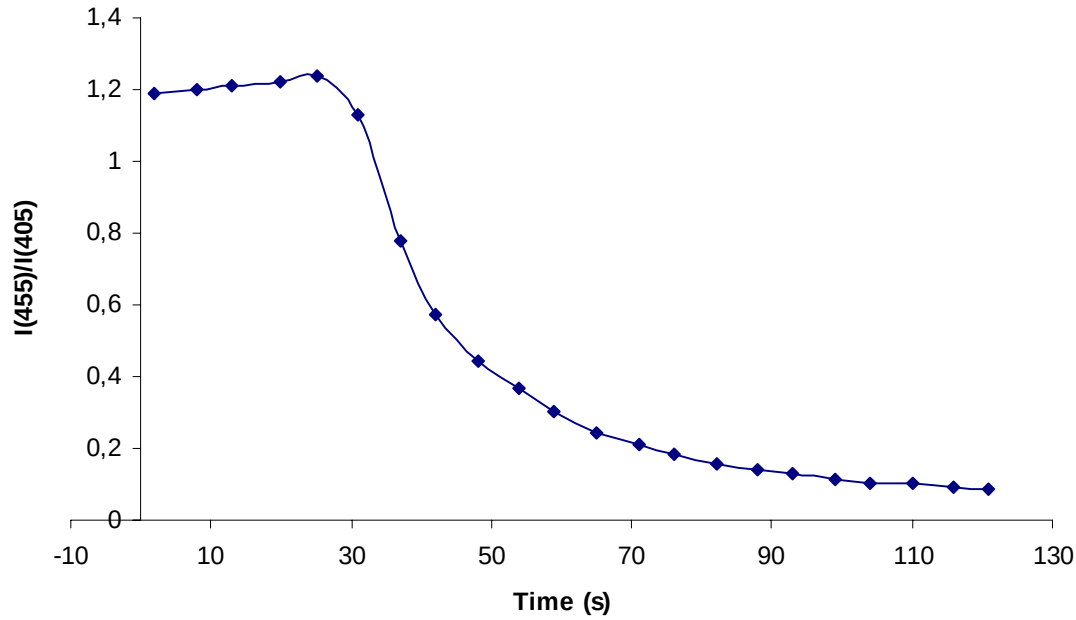

Figure 21. I_{405}/I_{455} corresponding to the titration of a buffer droplet with acetic acid, 10 µM.

3.3. Calculation of pH According to I_{405}/I_{455}

The HAc addition to the levitated droplet was performed at a rate of 10 Hz to the buffer levitaded droplet. The addition was triggered at 30 seconds after starting the

measurement. Knowing that the levitated droplet is 1 µL in volume and the concentration of the HAc solution added is 10 mM, the pH can be estimated through time, Thus, exemplifying for time = 31s (1 second after the beginning of HAc addition):

$$C_i \times V_i = C_f \times V_f \Leftrightarrow 10\ mM \times (10\ droplets \times 65 \times 10^{-6}\ \mu L) = C_f \times (1\ \mu L + 10 \times 65 \times 10^{-6}\ \mu L) \Leftrightarrow C_f \approx 6.5\ \mu M$$

Therefore, simply by increasing the concentration of acetic acid in the buffer solution (in a common glass) while measuring the pH changes with the help of a pH meter, the corresponding variance of pH in the droplet can be estimated. The following curve is obtained:

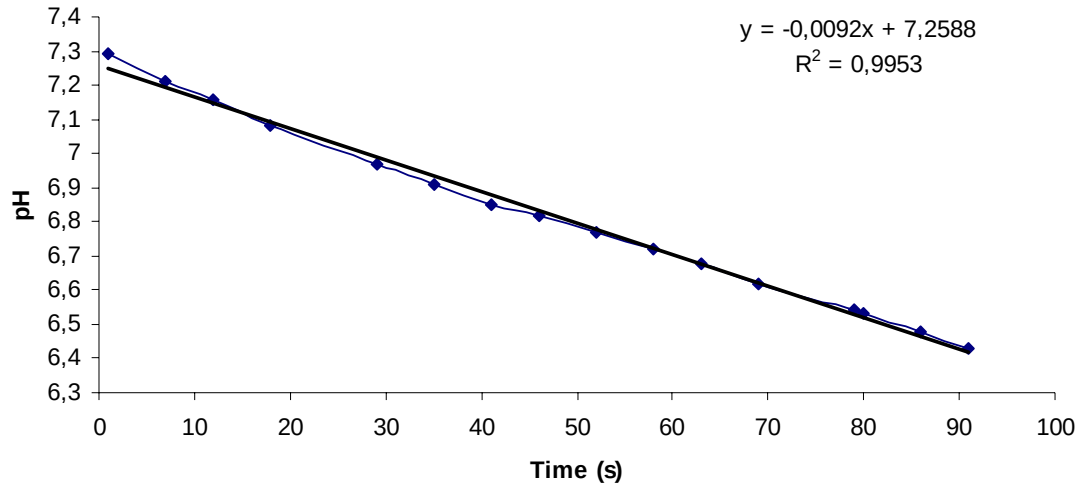

Figure 22. pH chances according time, during the titration of a buffer droplet with acetic acid, 10 µM.

3.4. Insulin Glycation

The non-enzymatic glycation of insulin can be divided in two different stages, the early and late Maillard reactions. The first stage consists in the formation of an

Amadori rearrangement product. The reactive carbonyl group of the sugar reacts with the nucleophilic amino group of the amino acid producing N-substituted glycosylamine and water. In the second stage advanced glycation end products (AGEs) are formed. They are a result of chemical reactions including oxidation, dehydration and condensation of the former product. The intermediate of both stages products are known, variously, as Amadori, Schiff bases and Maillard products.

Different methods could be used for following the glycation process. The early stage could be monitored by measuring the changes in absorbance at 350 nm based on the Shiff base formation[167]. The late Maillard reaction could be monitored by the spectro-fluorimetric method (λ_{ex} = 247 nm, λ_{em} = 420 nm) because of the fluorescent AGEs[168].

Besides the fluorescence and absorbance measurements of glycated proteins, immunological assays (ELISA) have been applied in the analysis of protein glycation[18]. All these methods did not provide sufficient quality information for precise monitoring of the process. This was due mainly to low sensitivity to detect the chemical changes throughout the reaction.

MALDI has already been successfully employed for the screening of enzymatic glycation of many proteins[169]. The application of MALDI-TOF-MS overcame the limitation in sensitivity and provided information at the human insulin glycation process based on changes in the mass of the protein.

3.4.1. MALDI-TOF Analysis of the Glycated Insulin

CHCA was used as a matrix and the results obtained in linear mode. With the help of the matrix, insulin, as well as all forms of glycated insulin, are ionized mainly with a single positive charge, yielding $[M+H]^+$. Nonetheless some double charged molecules $[M+2H]^{2+}$ can also be detected in the spectra.

Figure 23 shows the MALDI-TOF result of the products from the first to the sixteenth day of the glycation process.

a)

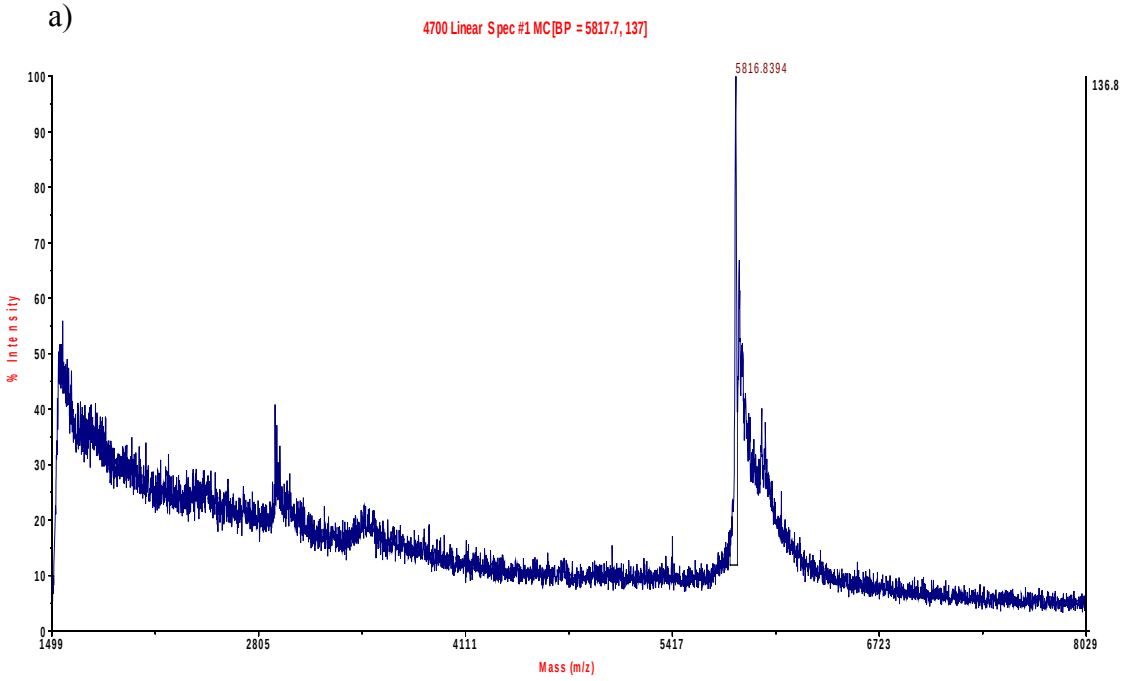
4700 Linear Spec #1 MC[BP = 5817.7, 137]
5816.8394
136.8
% Intensity
Mass (m/z)
1499
2805
4111
5417
6723
8029

b)

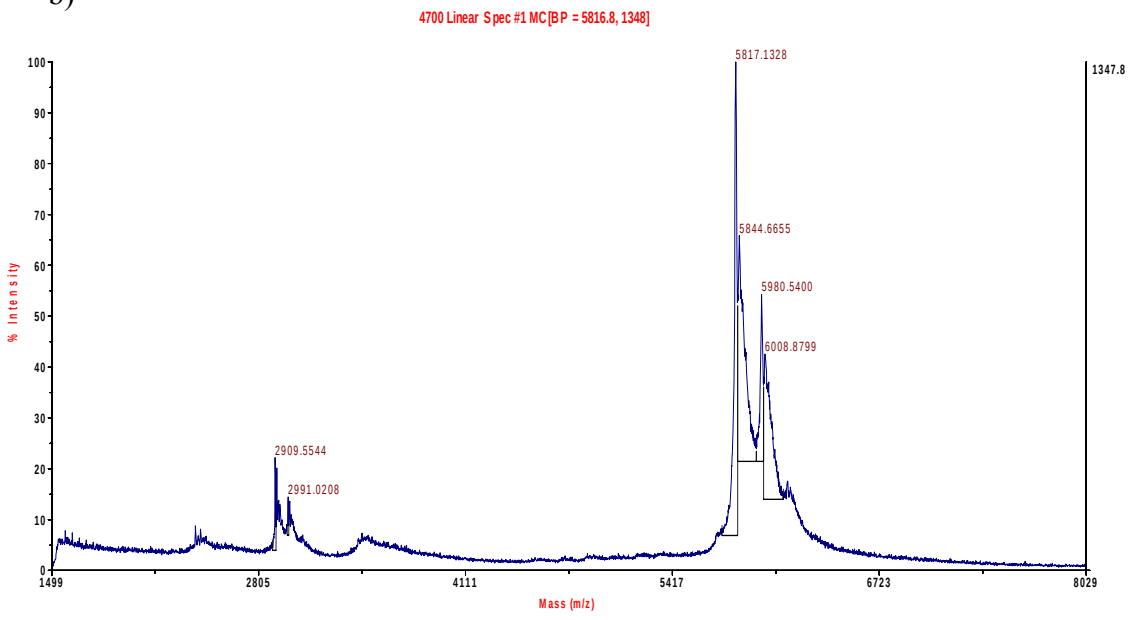
4700 Linear Spec #1 MC[BP = 5816.8, 1348]
5817.1328
1347.8
5844.6655
5980.5400
6008.8799
2909.5544
2991.0208
% Intensity
Mass (m/z)
1499
2805
4111
5417
6723
8029

c)

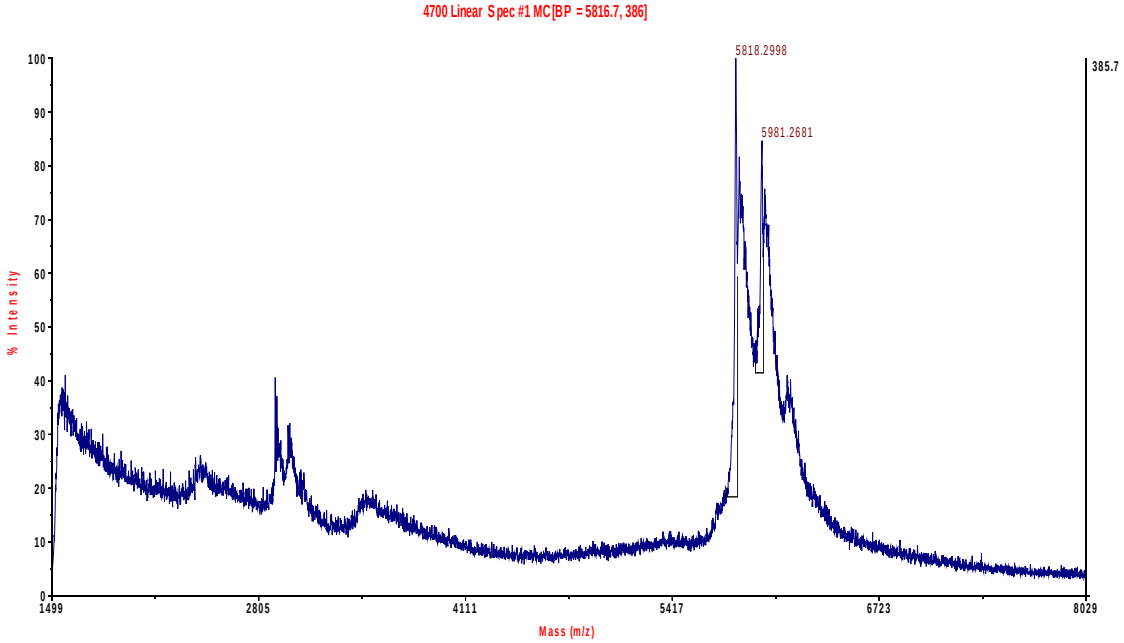
4700 Linear Spec #1 MC[BP = 5816.7, 386]
5818.2998
5981.2681
385.7
% Intensity
Mass (m/z)
1499
2805
4111
5417
6723
8029

d)

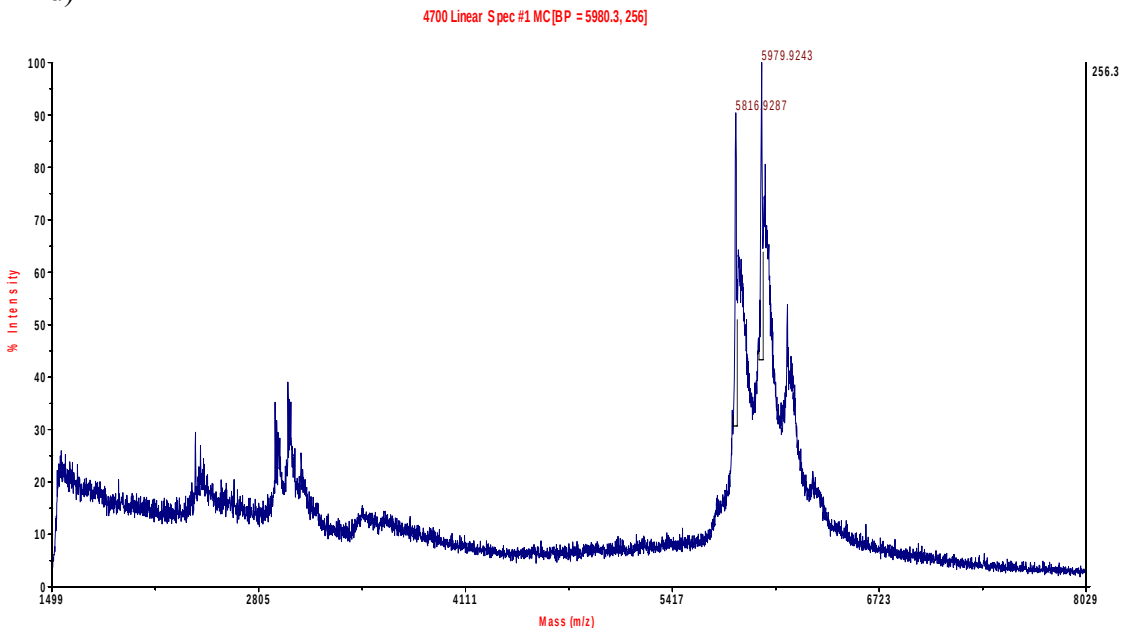
4700 Linear Spec #1 MC[BP = 5980.3, 256]
5979.9243
5816.9287
256.3
% Intensity
Mass (m/z)
1499
2805
4111
5417
6723
8029

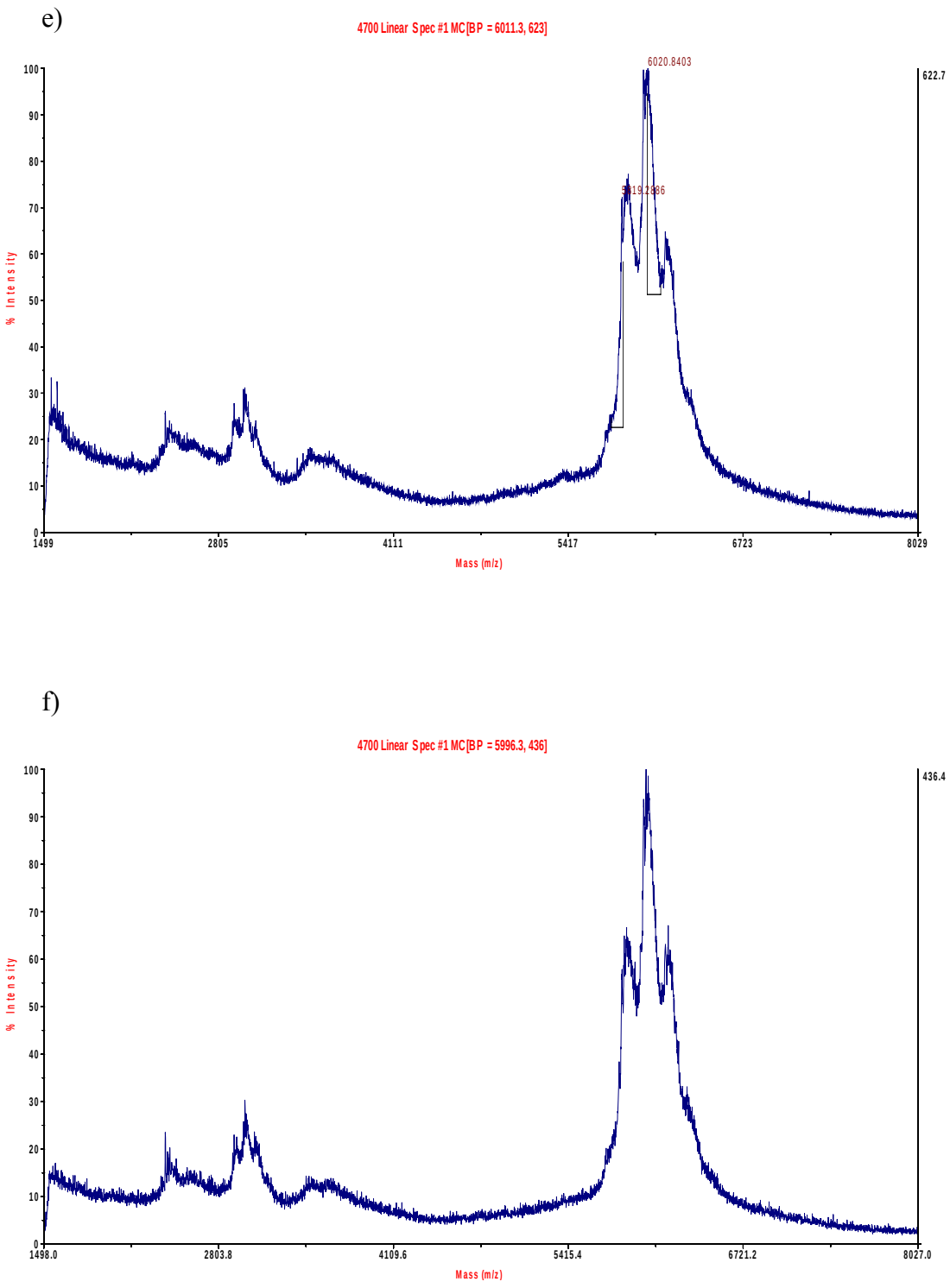

Figure 23. MALDI-TOF spectra of human insulin glycation product. (a) 1st day; (b) 4th day; (c) 7th day; (d) 10th day; (e) 13rd day; (f) 16th day.

Since the glycation rate depends on glucose concentration and time exposure to glucose, very high glucose concentration (1.6 M) and long incubation time (16 days) were employed.

The human insulin is not completely glycated in the reaction. However, it can be clearly seen the presence of mono-glycated, di-glycated and even tri-glycated insulin. If one compares the spectra through time, we can clearly see the occurrence of a peak at ~5.980 kDa corresponding to the mono-glycated insulin already after the first day of the whole glycation process. The appearance of a peak at ~ 6.145 kDa occurs already in the fourth day matching the di-glycated insulin.

In addition, the relative intensity of these peaks is growing stronger as the days go by. Thus, the peak for mono-glycated insulin rises above the one for non-glycated insulin in intensity already in the ninth day, whilst the peak for di-glycated insulin evens the non-glycated insulin peak out in intensity in the last day of the reaction.

One can also observe that a fourth peak starts to appear in the 10th day with a mass of approximately 6.310 kDa, which would match with the tri-glycated insulin. The difference in mass between the peaks is of about 165.7 Da which matches with the occurrence of one, two or even three glucitol adducts[170]. Should be noted that the interference of the noise was getting stronger as the days passed by. which suggested that the caramelization of the sugar must have occured till some extent in the insulin glycation process.

3.5. Few Cell Adipocyte Lipolysis

A 1-µL droplet containing about 10 adipocytes in the titration buffer with 10 µM HPTS was levitated at the nodal point of the standing wave in the acoustic levitator. The lipolysis was initiated with the addition of isoprenaline to a final concentration of 100 nM, leading to the release of FFAs out of the adipocytes and a consequent pH decrease in the surrounding buffer in the levitated droplet. Changes of pH in the droplet were detected using the pH-dependent fluorophore HPTS. The resulting changes in fluorescence intensity (I_{455} and I_{405}) during lipolysis are shown in fig. 24 and the correspondent intensity ratio (I_{455}/I_{405}) is shown in fig. 26. As expected, the fluorescence intensity decreased with the decrease in pH through time when exciting at 455 nm and

increased when exciting at 405 nm as shown in fig. 24. Therefore, the corresponding intensity ratio (I_{455}/I_{405}) decreased with the drop off of the pH value.

It is clear, that insulin is more effective stopping lipolysis than the glycated insulin. As shown in fig. 26, isoprenaline-induced lipolysis ceases earlier when inhibited with insulin than it is when inhibited with glycated insulin. This points for an important role of glycation of insulin in the development of type 2 diabetes

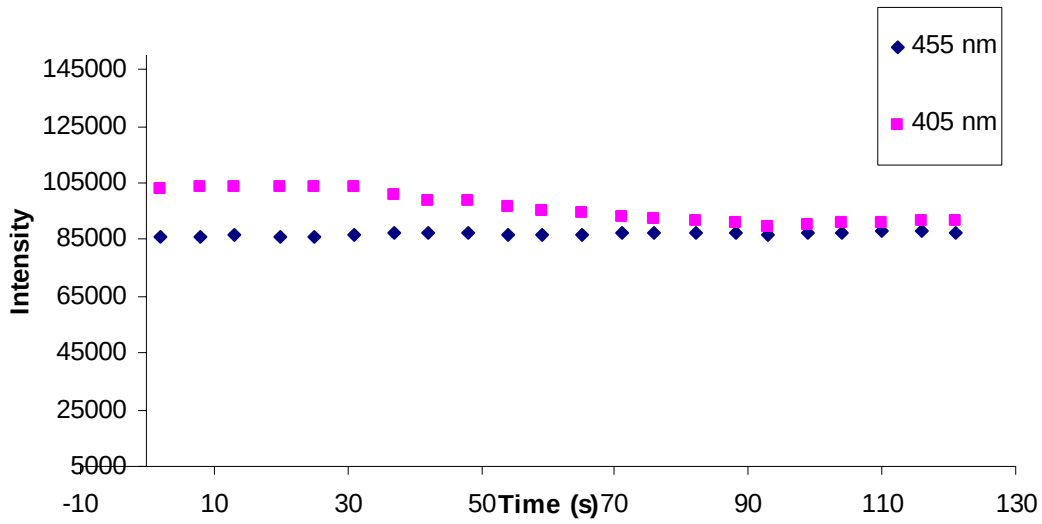

Figure 24. Fluorescence intensity (I_{435} and I_{405}) in the levitated droplet changes during adipocytes lipolysis process. The lipolisys was stoped with the addition of insulin at 90 s time.

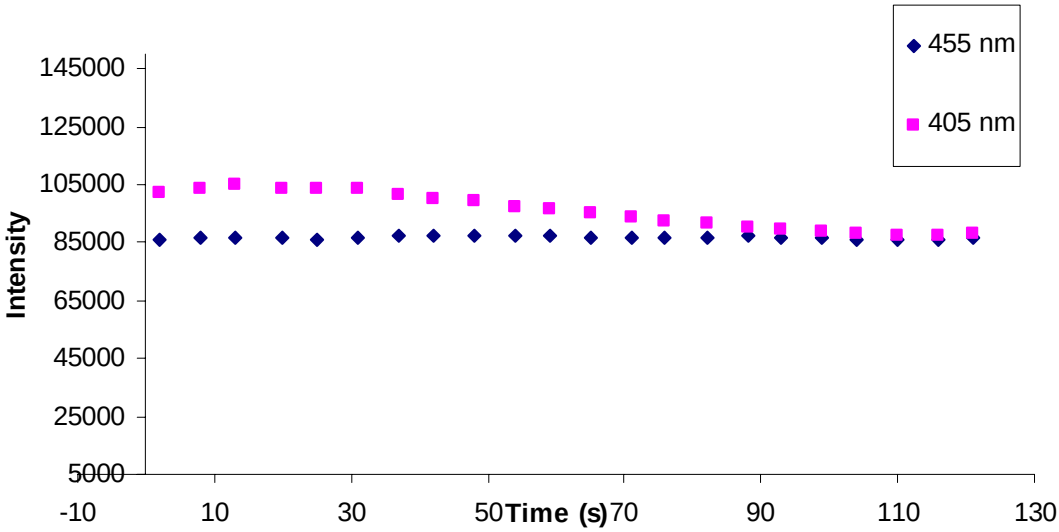

Figure 25. Fluorescence intensity (I_{435} and I_{405}) in the levitated droplet changes during adipocytes lipolysis process. The lipolisys was stoped with the addition of glycated insulin at 90 s time.

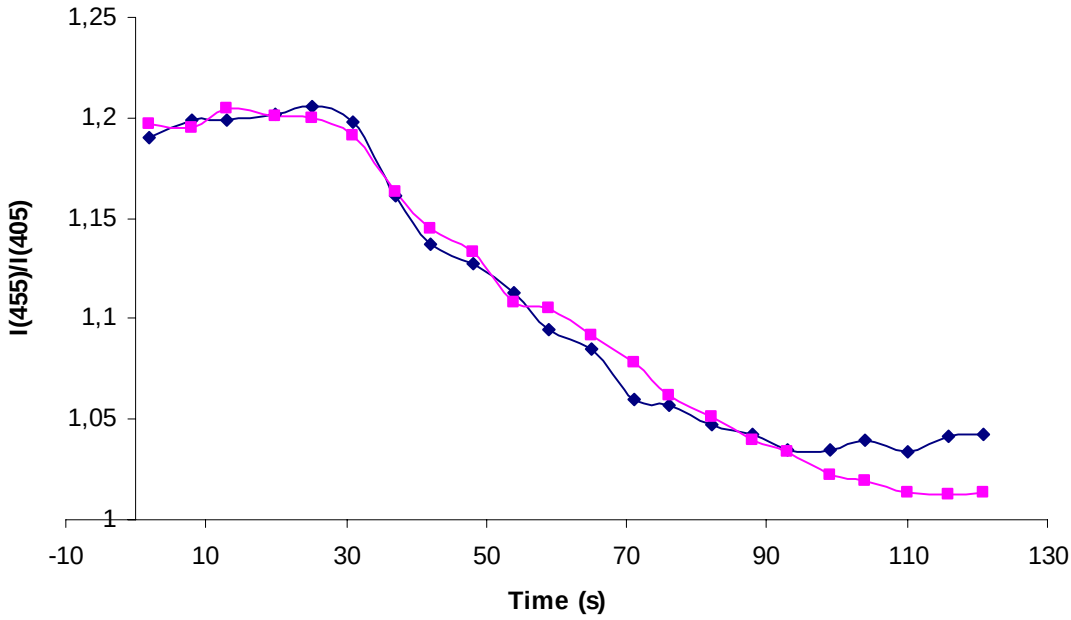

Figure 26. Fluorescence intensity ratio (I_{435}/I_{405}) in the levitated droplet during adipocytes lipolysis. Comparison between reactions stopped with the administration of insulin and glycated insulin to the levitated droplet.

3.6. MALDI Analysis of Lipolysis Stimulated Adipocytes

MALDI–TOF has become a widely used and powerful tool for the analysis of large peptides, biomolecules, and synthetic polymers. However, the typical spot-to-spot sample reproducibility and matrix interferences are still limiting factors. Another common limitation is the fact that the acquired spectra usually present complex features, because they are composed by a number of overlapping peaks with different amplitudes, related to the abundance of the proteins, and are contaminated by artifacts of biological/physical origin[171], i.e. the baseline trend and the background noise. Due to the presence of these disturbances, very sensitive and accurate peak-detection methods, able to correctly separate protein signals from noise, are required[172]. Regardless of the potential limitations, MALDI has many advantages including low detection limits that are in the attomole range.

Among the hormones synthesized and released from adipose tissue, which are somehow connected to the development of type 2 diabetes, are adiponectin, angiotensin, estradiol, IL-6, leptin, PAI-1, TNF-α, and resistin. The levels of adiponectin, for instance were found to be reduced in diabetics compared to non-diabetics, playing a role in the suppression of the metabolic derangements that may result in[51]. Another good example is resistin. It is believed that there are positive correlations between resistin levels and insulin resistance. Resistin may also be a link in the well-known association between inflammation and insulin resistance[53,54].

Thus, some of the cell-containing droplets collected after the fluorescence experiments were taken to MALDI detection. Few peaks could be systematically detected (fig. 27). However, we were not able, so far, to identify them. Hence, more efforts are required in order to achieve this aim.

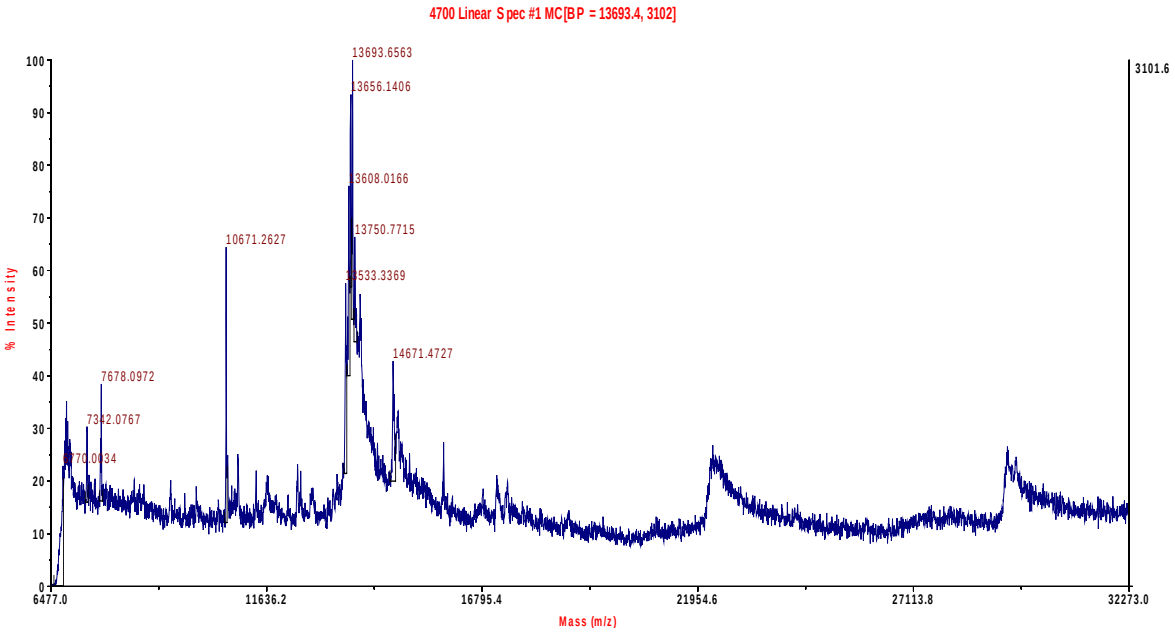

Figure 27. MALDI-TOF spectra of adipocytes subjected to lipolysis stimulation.

4. Conclusions

The applicability of the *airborne system,* interfaced with fluorescence imaging detection and MALDI, towards cell metabolism studies at the single/few cell level has been shown.

The system has been applied using cells of significance for type 2 diabetes related research. Adipocyte lipolysis was detected at the few-cell level using fluorescence imaging detection. The system proved to be sensitive to differences in the lipolytic response under different experimental conditions. Isoprenaline-induced lipolysis in a cell containing levitated drop, in real time, resulted in the decrease of pH in the surrounding buffer.

Moreover, insulin has been successfully administrated to stop adipocyte lipolysis induced by isoprenaline. In comparison, the application of glycated insulin showed not to be so effective in the endeavour of stopping lipolysis in the same conditions, which is an important finding in the context of type 2 diabetes.

Mainly because of its distinctive sensitivity, the developed methodology brings great value for single cell studies. Furthermore it can be easily adapted to other cell systems and reactions.

Yet, the airborne system can be of great convenience when the amount of sample available is rather low as is usually the case of cells obtained from, for example, human biopsies.

5. Future Outlook

5.1. Real-time Experiments

The Airborne System is currently interfaced off-line to MALDI-TOF-MS. So far, freshly prepared primary cells, single-cell response, cell-cell communications, and the behavior of simple mixed cell populations have been studied as a function of various stimuli. Currently, a particular cellular system is allowed to evolve for a well-defined time period, and then the entire levitated droplet is extracted onto a MALDI plate for analysis in a high-resolution MALDI TOF/TOF instrument. Although, we are learning a lot from these "dead end" analyses, acquiring each data point currently requires the inconvenient re-initiation of the whole experiment with a new levitated drop and fresh cellular contents.

An important technical goal of the present project is therefore to develop techniques which can interrogate and monitor analytes of interest in a levitated droplet, non-destructively, on-demand, and over extended periods of time, by MS.

The specific setups shown in fig. 28, which require a *lateral* extraction of ions, are dictated by the construction of the levitator. We believe that the levitator can be more conveniently and flexibly coupled to mass analyzers and other ion processing tools like field-asymmetric ion mobility spectrometry (FAIMS, explored for MS sensitivity enhancement and analyte separations, Mie *et al.*[173,174]) if charged species can be extracted *axially* from the levitator, as shown in fig. 28.e). The levitators at our disposal are of an open construction which will allow us to experiment with alternative schemes for extracting ions.

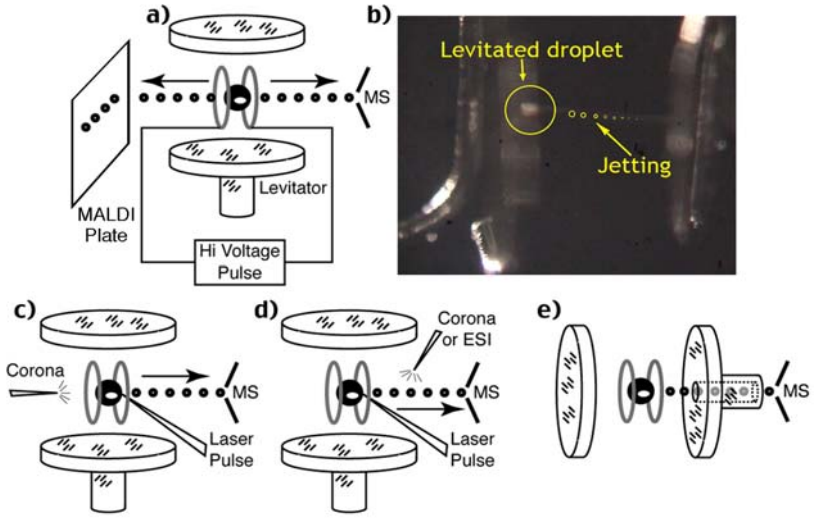

Figure 28. Schemes for monitoring levitated droplets with mass spectrometry (MS). a) A droplet is levitated between two ring electrodes to which high voltage pulses are applied. Polarization and emission of progeny droplets occur and the latter are sampled into an MS or deposited onto a sample plate for MALDI-MS. b) The droplet "spitting" process observed. c) Levitated droplets can be charged by a corona discharge and then subjected to a laser pulse to desorb small charged droplets for MS. d) Small droplets can be desorbed from a levitated droplet by a laser pulse and these droplets ionized for subsequent MS analysis by a corona or electrospray plume. e) An axial scheme for extraction of charged progeny droplets from the levitator may allow more convenient interface to MS.

5.2. Insulin Mimetic Compounds

In collaboration with Ebbe Nordlander from Chemical Physical Department at Lund University, we aim to test a few insulin mimetic drugs by using the same system that has been used to promote/stop lipolysis in adipocytes. These drugs are thought to mimic several insulin effects in the cells.

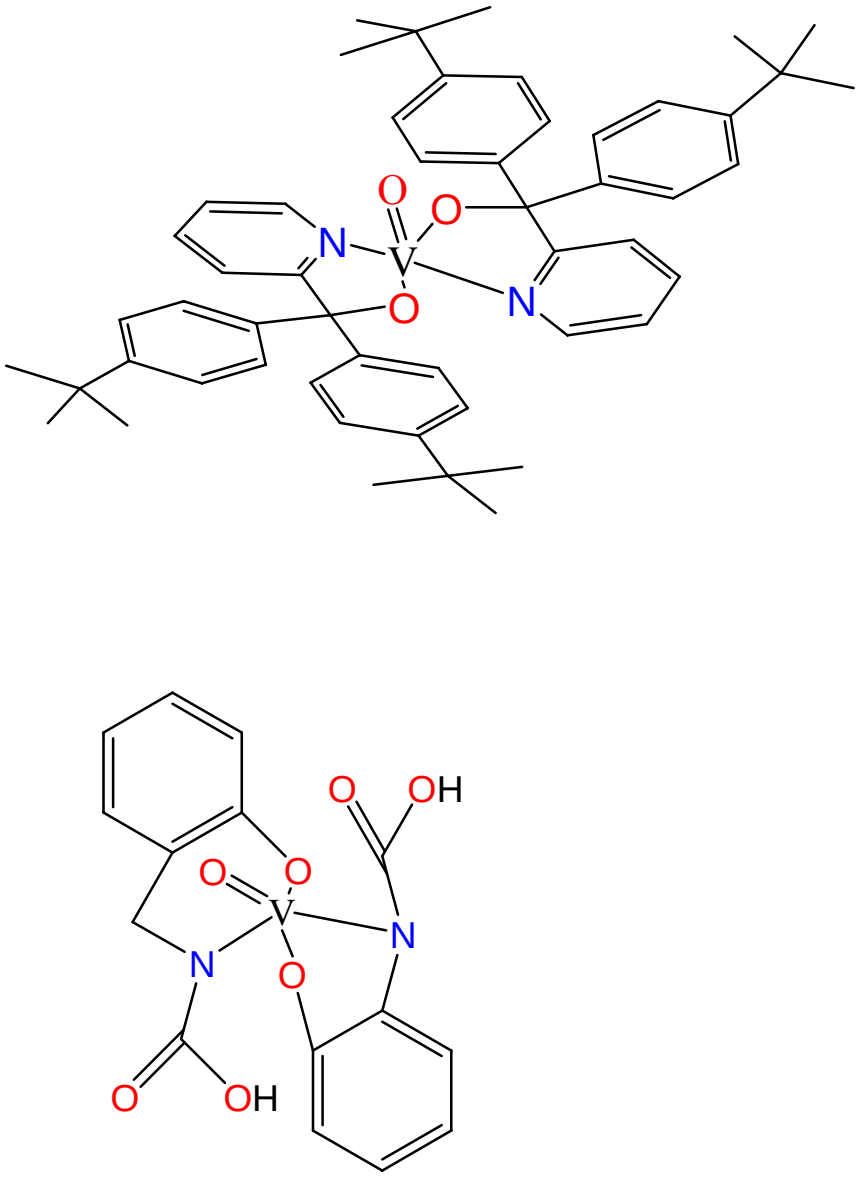

Figure 29. Chemical structure of insulin mimetic drugs to be tested in the fluorescence system together with the adipocytes

6. References

1. Santesson, S.D., E.; Rorsman, P.; Johansson, T.; Lemos, S.; Nilsson, S. . Cell-Cell Communication between Adipocytes and Pancreatic β-Cells in Acoustically Levitated Droplets. *Integrative Biology* **DOI:10.1039/b907834g**(2009).
2. Nilsson, S.J.P., M. I.; Schweitz, L.; Johansson, T. L. L. . 36th Annual Eastern Analytical Symposium & Exposition, Somerset, NJ, USA. (1997).
3. Laurell, T.N.S., S.; Nilsson, S.; Zivin, R.; Thurmond, R.; Patel, L. . System for Performing Assays on a Levitated Droplet. **US Patent WO 99/44746** (1999).
4. Zimmet, P.A., K. G. M. M.; Shaw, J. Global and societal implications of the diabetes epidemic. *Nature* **414**, 782-787 (2001).
5. Norhammar, A.T., A.; Nilsson, G.; Hamsten, A.; Efendic, S.; Ryden, L.; Malmberg, K. Glucose metabolism in patients with acute myocardial infarction and no previous diagnosis of diabetes mellitus: a prospective study. *Lancet* **359**, 2140-2144 (2002).
6. Weber, M.B.N., K.M.V. Preventing type 2 diabetes: Genes or lifestyle? *Primary Care Diabetes* **2**, 65-66 (2008).
7. Robertson, R.P.H., J.; Tran, P. O.; Tanaka, Y.; Takahashi, H. Glucose toxicity in b-cells: Type 2 diabetes, good radicals gone bad, and the glutathione connection. *Diabetes* **52**, 581-587 (2003).
8. Knowler, W.C.B.-C., E.; Fowler, S. E.; Hamman, R. F.; Lachin, J. M.; Walker, E. A.; Nathan, D. M. Reduction in the incidence of type 2 diabetes with lifestyle intervention or metformin. *The New England Journal of Medicine* **346**, 393-403 (2002).
9. Minokoshi, Y.K., C.; Kahn, B. Tissue-specific Ablation of the GLUT4 Glucose Transporter or the Insulin Receptor Challenges Assumptions about Insulin Action and Glucose Homeostasis. *The Journal of Biological Chemistry* **278**, 33609–33612 (2003).
10. O'Harte, F.P.M., Hojrup, P., Barnett, C.R. & Flatt, P.R. Identification of the Site of Glycation of Human Insulin. *Peptides* **17**, 1323-1330 (1996).
11. Hunter, S.J. et al. Demonstration of Glycated Insulin in Human Diabetic Plasma and Decreased Biological Activity Assessed by Euglycemic-Hyperinsulinemic Clamp Technique in Humans. *Diabetes* **52**, 492-498 (2003).
12. Abdel-Wahab, Y.H.A., O'Harte, F.P.M., Boyd, A.C., Barnett, C.R. & Flatt, P.R. Glycation of insulin results in reduced biological activity in mice. *Acta Diabetologica* **34**, 265-270 (1997).
13. Boyd, A.C. et al. Impaired ability of glycated insulin to regulate plasma glucose and stimulate glucose transport and metabolism in mouse abdominal muscle. *Biochimica et Biophysica Acta (BBA)/General Subjects* **1523**, 128-134 (2000).
14. STITT, A.W. Advanced glycation: an important pathological event in diabetic and age related ocular disease. *British Journal of Ophthalmology* **85**, 746-753 (2001).
15. Abdel-Wahab, Y.H.A., O'Harte, F.P.M., Barnett, C.R. & Flatt, P.R. Characterization of insulin glycation in insulin-secreting cells maintained in tissue culture. *J Endocrinol* **152**, 59-67 (1997).

16. Lindsay, J.R. et al. Effects of nateglinide on the secretion of glycated insulin and glucose tolerance in type 2 diabetes. *Diabetes research and clinical practice* **61**, 167-173 (2003).
17. O'Harte, F.P.M. et al. Structure, antihyperglycemic activity and cellular actions of a novel diglycated human insulin. *Peptides* **21**, 1519-1526 (2000).
18. Farah, M.A., Bose, S., Lee, J.-H., Jung, H.-C. & Kim, Y. Analysis of glycated insulin by MALDI-TOF mass spectrometry. *Biochimica et Biophysica Acta (BBA) - General Subjects* **1725**, 269-282 (2005).
19. Lindsay, J.R. et al. Demonstration of increased concentrations of circulating glycated insulin in human Type 2 diabetes using a novel and specific radioimmunoassay. *Diabetologia* **46**, 475-478 (2003).
20. Brunicardi, F.C.S., D. M.; Andersen, D. K. . Neural regulation of the endocrine pancreas. *International journal of pancreatology* **18**, 177-95 (1995).
21. Gilon, P.H., J. C. . Mechanisms and physiological significance of the cholinergic control of the pancreatic β-cell function. *Endocrine Reviews* **22**, 565-604 (2001).
22. Henquin, J.C.R., M. A.; Nenquin, M.; Jonas, J. C.; Gilon, P. Hierarchy of the B-cell signals controlling insulin secretion. *European Journal of Clinical Investigation* **33**, 742–750 (2003).
23. Jones, P.M.P., S. J. . Protein kinases, protein phosphorylation, and the regulation of insulin secretion from pancreatic β-cells. *Endocrine Reviews* **19**, 429-461 (1998).
24. Komatsu, M.S., T.; Aizawa, T.; Sharp, G. W. G Glucose stimulation of insulin release in the absence of extracellular Ca2+ and in the absence of any increase in intracellular Ca2+ in rat pancreatic islets. *Proceedings of the National Academy of Sciences of the USA* **92**, 10728-10732 (1995).
25. Carmen, G.-Y. & Víctor, S.-M. Signalling mechanisms regulating lipolysis. *Cellular Signalling* **18**, 401-408 (2006).
26. Saloranta, C., Franssila-Kallunki, A., Ekstrand, A., Taskinen, M.R. & Groop, L. Modulation of hepatic glucose production by non-esterified fatty acids in Type 2 (non-insulin-dependent) diabetes mellitus. *Diabetologia* **34**, 409-415 (1991).
27. Taniguchi, C.M., Emanuelli, B. & Kahn, R. Critical nodes in signalling pathways: insights into insulin action. *Nature Reviews Molecular Cell Biology* **7**, 85-97 (2006).
28. John, J.E. et al. Mechanism of Hormone-Stimulated Lipolysis in Adipocytes: Translocation of Hormone-Sensitive Lipase to the Lipid Storage Droplet. *Proceedings of the National Academy of Sciences of the United States of America* **89**, 8537-8541 (1992).
29. Gasic, S., Tian, B. & Green, A. Tumor Necrosis Factor alpha Stimulates Lipolysis in Adipocytes by Decreasing Gi Protein Concentrations. *J. Biol. Chem.* **274**, 6770-6775 (1999).
30. Pinkney, J.H., Coppack, S.W. & Mohamed-Ali, V. Effect of isoprenaline on plasma leptin and lipolysis in humans. *Clinical Endocrinology* **48**, 407-411 (1998).
31. Masahiro, K. et al. Hormone-Sensitive Lipase in Differentiated 3T3-L1 Cells and Its Activation by Cyclic AMP-Dependent Protein Kinase. *Proceedings of the National Academy of Sciences of the United States of America* **78**, 732-736 (1981).
32. Blasiole, D.a.D., RA and Attie,AD The physiological and molecular regulation of lipoprotein assembly and secretion. *Mol Biosyst* **3**, 608-19 (2007).

33. Horowitz, J.F. & Klein, S. Whole body and abdominal lipolytic sensitivity to epinephrine is suppressed in upper body obese women. *Am J Physiol Endocrinol Metab* **278**, E1144-1152 (2000).
34. Blaak, E.E. Fatty acid metabolism in obesity and type 2 diabetes mellitus. *Proceedings of the Nutrition Society* **62**, 753-760 (2003).
35. Defronzo, R.A. Dysfunctional fat cells, lipotoxicity and type 2 diabetes. *International Journal of Clinical Practice* **58**, 9-21 (2004).
36. Monetti, M. et al. Dissociation of Hepatic Steatosis and Insulin Resistance in Mice Overexpressing DGAT in the Liver. **6**, 69-78 (2007).
37. Chibalin, A.V. et al. Downregulation of Diacylglycerol Kinase Delta Contributes to Hyperglycemia-Induced Insulin Resistance. **132**, 375-386 (2008).
38. Kahn, S.E., Hull, R.L. & Utzschneider, K.M. Mechanisms linking obesity to insulin resistance and type 2 diabetes. *Nature* **444**, 840-846 (2006).
39. Shoelson, S.E. Inflammation and insulin resistance. *The Journal of Clinical Investigation* **116**, 1793-1801 (2006).
40. Blüher, M. et al. Adipose Tissue Selective Insulin Receptor Knockout Protects against Obesity and Obesity-Related Glucose Intolerance. **3**, 25-38 (2002).
41. Lundgren, M. et al. Fat cell enlargement is an independent marker of insulin resistance and `hyperleptinaemia'. Vol. 50 625-633 (2007).
42. Danforth, E. Failure of adipocyte differentiation causes type II diabetes mellitus? *Nature Genetics* **26**, 13-14 (2000).
43. McLaughlin, T. et al. Enhanced proportion of small adipose cells in insulin-resistant vs insulin-sensitive obese individuals implicates impaired adipogenesis. Vol. 50 1707-1715 (2007).
44. Spalding, K.L. et al. Dynamics of fat cell turnover in humans. *Nature* **453**, 783-787 (2008).
45. Weisberg, S.P., McCann, D., Desai, M., Rosenbaum, M., Leibel, R.L., and Ferrante, A.W. Obesity is associated with macrophage accumulation in adipose tissue. *J Clin Invest* **112**, 1796-1808
(2003).
46. Hotamisligil, G.S.A., P.; Caro, J. F.; Atkinson, R. L.; Spiegelman, B. M. Increased adipose tissue expression of tumor necrosis factor-alpha in human obesity and insulin resistance. *J Clin Invest.* **95**, 2409-2415 (1995).
47. Kristiansen, O.P.M.-P., T. Interleukin-6 and Diabetes: The Good, the Bad, or the Indifferent? *Diabetes* **54**, S114-S124 (2005).
48. Febbraio, M.A. gp130 receptor ligands as potential therapeutic targets for obesity. *J. Clin. Invest.* **117**, 841-849 (2007).
49. Attie, A.D. & Scherer, P.E. Adipocyte metabolism and obesity. *J. Lipid Res.* **50**, S395-399 (2009).
50. Wang, M.-y., Orci, L., Ravazzola, M. & Unger, R.H. Fat storage in adipocytes requires inactivation of leptin's paracrine activity: Implications for treatment of human obesity. *Proceedings of the National Academy of Sciences of the United States of America* **102**, 18011-18016 (2005).
51. Duncan, B.B.S., M. I.; Pankow, J. S.; Bang, H.; Couper, D.; Ballantyne, C. M.; Hoogeveen, R. C.; Heiss, G. . Adiponectin and the Development of Type 2 Diabetes. *Diabetes* **53**, 2473-2478. (2004).
52. Kim, J.-Y. Obesity-associated improvements in metabolic profile through expansion of adipose tissue. *The Journal of Clinical Investigation* **117**, 2621-2637 (2007).

53. *Ehtesham, N.Z.* Molecular link between diabetes and obesity: The resistin story. *Current Science* **80**, 1369 (2001).
54. Steppan, C.M.B., S. T.; Bhat, S.; Brown, E. J.; Banerjee, R. R.; Wright, C. M.; Patel, H. R.; Ahima, R. S.; Lazar, M. A. The hormone resistin links obesity to diabetes. *Nature* **409**, 307-12 (2001).
55. Milan, G. et al. Resistin and Adiponectin Expression in Visceral Fat of Obese Rats: Effect of Weight Loss. *Obesity* **10**, 1095-1103 (2002).
56. Silswal, N. et al. Human resistin stimulates the pro-inflammatory cytokines TNF-@a and IL-12 in macrophages by NF-@kB-dependent pathway. *Biochemical and Biophysical Research Communications* **334**, 1092-1101 (2005).
57. Wellen, K.E. & Hotamisligil, G.k.S. Inflammation, stress, and diabetes. *The Journal of Clinical Investigation* **115**, 1111-1119 (2005).
58. Janasek, D.F., J.; Manz, A. Scaling and the design of miniaturized chemical-analysis systems. *Nature* **442**, 374-380 (2006).
59. Priego-Capote, F.d.C., L. Ultrasound-assisted levitation: Lab-on-a-drop. *Trends in Analytical Chemistry* **25**, 856-867 (2006).
60. Santesson, S.N., S. Airborne chemistry: acoustic levitation in chemical analysis. *Analytical and Bioanalytical Chemistry* **378**, 1704-1709 (2004).
61. Welter, E.N., B. Acoustically levitated droplets – a new tool for micro and trace analysis. *Fresenius Journal of Analytical Chemistry* **357**, 345-350 (1997).
62. Biswas, A. Solidification of acoustically levitated o-terphenyl crystals: A Raman study. *Journal of Crystal Growth* **147**, 155-164 (1995).
63. Santesson, S.C.-Z., E. S.; Johansson, T.; Laurell, T.; Nilsson, J.; Nilsson, S. Screening of Nucleation Conditions Using Levitated Drops for Protein Crystallization. *Analytical Chemistry* **75**, 1733-1740 (2003).
64. Brenn, G., Deviprasath, L.J., Durst, F. & Fink, C. Evaporation of acoustically levitated multi-component liquid droplets. *International Journal of Heat and Mass Transfer* **50**, 5073-5086 (2007).
65. Tuckermann, R., Bauerecker, S. & Cammenga, H.K. IR-Thermography of Evaporating Acoustically Levitated Drops. Vol. 26 1583-1594 (2005).
66. Tuckermann, R., Bauerecker, S. & Cammenga, H.K. Generation and characterization of surface layers on acoustically levitated drops. *Journal of Colloid and Interface Science* **310**, 559-569 (2007).
67. Biedasek, S., Abboud, M., Moritz, H.-U. & Stammer, A. Online-Analysis on Acoustically Levitated Droplets. *Macromolecular Symposia* **259**, 390-396 (2007).
68. Leiterer, J., Emmerling, F., ThÃ¼nemann, A.F. & Panne, U. Characterisation of levitated samples for modelling of condensed matter. Vol. 632 2132-2132 (2006).
69. Santesson, S.A., M.; Degerman, E.; Johansson, T.; Nilsson, J.; Nilsson, S. Airborne cell analysis. *Analytical Chemistry* **72**, 3412-3418 (2000).
70. Brandt, E.H. Suspende by sound. *Nature* **413**, 474-475 (2001).
71. Vandaele, V.L., P.; Delchambre, A. Non-contact handling in microassembly: Acoustical levitation. *Precision Engineering* **29**, 491-505 (2005).
72. Bücks, K. & Müller, H. *Z. Phys.* **84**, 75-86 (1933).
73. Rohling, O.W., C.; Neidhart, B. Experimental setup for the determination of analytes contained in ultrasonically levitated drops. *Fresenius Journal of Analytical Chemistry* **368**, 125-129 (2000).

74. Lierke, E.G. Acoustic levitation - A comprehensive survey of principles and applications. *Acustica* **82**, 220-237 (1996).
75. Anilkumar, A.V.L., C. P.; Wang, T. G. Stability of an acoustically levitated & flattened drop: an experimental study. *Physics of Fluids A: Fluid Dynamics* **5**, 2763-2774 (1993).
76. Yarin, A.L.W., D.A.; Brenn, G.; Rensink, D. Acoustically levitated drops: drop oscillation and break-up driven by ultrasound modulation. *International Journal of Multiphase Flow* **28**, 887-910 (2002).
77. Oennerfjord, P.N., J.; Wallman, L.; Laurell, T.; Marko-Varga, G. Picoliter Sample Preparation in MALDI-TOF MS Using a Micromachined Silicon Flow-Through Dispenser. *Analytical Chemistry* **70**, 4755-4760 (1998).
78. Laurell, T.W., L.; Nilsson, J. Design and development of a silicon microfabricated flow-through dispenser for on-line picolitre sample handling. *Journal of Micromechanics and Microengineering* **9**, 369-376 (1999).
79. Jacob, P.S., A.; Hergenroder, R.; Klockow, D. Phase transfer and freezing processes investigated on acoustically levitated aqueous droplets. *Fresenius Journal of Analytical Chemistry* **371**, 726-733 (2001).
80. Xu, T., Jin, J., Gregory, C., Hickman, J.J. & Boland, T. Inkjet printing of viable mammalian cells. *Biomaterials* **26**, 93-99 (2005).
81. Demirci, U.M., G. Single cell epitaxy by acoustic picolitre droplets. *Lab Chip.* **7**, 1139-45 (2007).
82. Petersson, M.N., J.; Wallman, L.; Laurell, T.; Johansson, J.; Nilsson, S. Sample enrichment in a single levitated droplet for capillary electrophoresis. *Journal of Chromatography B: Biomedical Sciences and Applications* **714**, 39-46 (1998).
83. Weis, D.D.N., J. D. Enzyme Kinetics in Acoustically Levitated Droplets of Supercooled Water: A Novel Approach to Cryoenzymology. *Analytical Chemistry* **77**, 2558-2563 (2005).
84. Santesson, S.R., I. B.-R.; Viberg, P.; Jergil, B.; Nilsson, S. Affinity Two-Phase Partitioning in Acoustically Levitated Drops. *Analytical Chemistry* **76**, 303-308 (2004).
85. Esen, C.W., T.; Sprynchak, V.; Schweiger, G. Raman spectroscopy on deformed droplets: theory and experiment. *Journal of Quantitative Spectroscopy and Radiative Transfer* **89**, 79-85 (2004).
86. Omrane, A.S., S.; Aldén, M.; Nilsson, S. Laser techniques in acoustically levitated micro droplets. *Lab on a Chip* **4**, 287-291 (2004).
87. Santesson, S.J., J.; Taylor, L. S.; Levander, I.; Fox, S.; Sepaniak, M.; Nilsson, S. Airborne Chemistry Coupled to Raman Spectroscopy. *Analytical Chemistry* **75**, 2177-2180 (2003).
88. Cerenius, Y.O., A.; Santesson, S.; Nilsson, S.; Kloo, L. Preliminary tests on the use of an acoustic levitator for liquid X-ray diffraction experiments. *Journal of Applied Crystallography* **36**, 163-164 (2003).
89. Leiterer, J.D.e., F.; Emmerling, F.; Thünemann, A. F.; Panne, U. Structure analysis using acoustically levitated droplets. *Analytical and Bioanalytical Chemistry* **391**, 1221-1228 (2008).
90. Kawahara, N.Y., A. L.; Brenn, G.; Kastner, O.; Durst, F. Effect of acoustic streaming on the mass transfer from a sublimating sphere. *Physics of Fluids* **12**, 912 (2000).
91. Trinh, E.H.R., J. L. Experimental Study of Streaming Flows Associated with Ultrasonic Levitators. *Physics of Fluids* **6**, 3567-3579 (1994).

92. Yarin, A.L.B., G.; Kastner, O.; Rensink, D.; Tropea, C. Evaporation of acoustically levitated droplets. *Journal of fluid mechanics* **399**, 151-204 (1999).
93. Schiffter, H.L., G. Single-droplet evaporation kinetics and particle formation in an acoustic levitator. Part 2: Drying kinetics and particle formation from microdroplets of aqueous mannitol, trehalose, or catalase. *Journal of Pharmaceutical Sciences* **96**, 2284-2295 (2007).
94. Nilsson, S.J., J. S. E.; Petersson, M. I.; Schweitz, L.; Johansson, T. L. L. . 36th Annual Eastern Analytical Symposium & Exposition, Somerset, NJ, USA. (1997).
95. Laurell, T.N., J.; Santesson, S.; Nilsson, S.; Zivin, R.; Thurmond, R.; Patel, L., 1999]. System for Performing Assays on a Levitated Droplet. **US Patent WO 99/44746** (1999).
96. Santesson, S. Miniaturised Bioanalytical Chemistry in Acoustically Levitated Droplets. *Doctoral Dissertation* **ISBN 91-628-6093-3**(2004).
97. Lakowicz, J.R. *Principles of fluorescence spectroscopy*, (Springer, New York, 2006).
98. Freudenberg, S. et al. Fluorescence microscopic investigation of Aspergillus awamori growing on synthetic and complex media and producing xylanase. *Journal of Biotechnology* **46**, 265-273 (1996).
99. Tanner, M.K. & Wellhausen, S.R. Flow Cytometric Detection of Fluorescent Redistributional Dyes for Measurement of Cell Transmembrane Potential. Vol. 91 85-95 (1997).
100. Andersson-Engels, S., Johansson, J. & Svanberg, S. Medical diagnostic system based on simultaneous multispectral fluorescence imaging. *Appl. Opt.* **33**, 8022-8029 (1994).
101. Karger, A.E., Harris, J.M. & Gesteland, R.F. Multiwavelength fluorescence detection for DNA sequencing using capillary electrophoresis. *Nucl. Acids Res.* **19**, 4955-4962 (1991).
102. Farber, S.A. et al. Genetic Analysis of Digestive Physiology Using Fluorescent Phospholipid Reporters. *Science* **292**, 1385-1388 (2001).
103. Stokes, G.G. On the Change of Refrangibility of Ligh. *Philosophical Transactions of the Royal Society of London* **142**, 463-562 (1852).
104. Williams, A.T.R.W., Stephen A.; Miller, James N. . Relative fluorescence quantum yields using a computer-controlled luminescence spectrometer. *The Analyst* **108**, 1067 (1983).
105. Tsien, R.Y. & Poenie, M. Fluorescence ratio imaging: a new window into intracellular ionic signaling. *Trends in Biochemical Sciences* **11**, 450-455 (1986).
106. Stromberg, N. & Hulth, S. Time correlated pixel-by-pixel calibration for quantification and signal quality control during solute imaging. *Sensors and Actuators B: Chemical* **115**, 263-269 (2006).
107. Stromberg, N. & Hulth, S. Assessing an imaging ammonium sensor using time correlated pixel-by-pixel calibration. *Analytica Chimica Acta* **550**, 61-68 (2005).
108. Tsien, R., Rink, T. & Poenie, M. Measurement of cytosolic free Ca²⁺ in individual small cells using fluorescence microscopy with dual excitation wavelengths. *Cell Calcium* **6**, 145-157 (1985).
109. Lerson, T., McNeil, P., Reynolds, G.T. & Taylor, D.L. Microspectrofluorometry by Digital Image Processing: Measurement of Cytoplasmic pH. *The Journal of Cell Biology* **98**, 717-724 (1984).

110. Strömberg, N., Mattsson, E. & Hakonen, A. An imaging pH optode for cell studies based on covalent attachment of 8-hydroxypyrene-1,3,6-trisulfonate to amino cellulose acetate films. *Analytica Chimica Acta* **636**, 89-94 (2009).
111. Heiple, J.M.T., D. L. An optical technique for measurement of intracellular pH in single living cells. *Kroc Found Ser* **15**, 21-54 (1981).
112. Nuccitelli, R. Intracellular pH measurement techniques: their advantages and limitations. *Kroc Found Ser* **15**, 161-9 (1981).
113. Ohkuma, S. & Poole, B. Fluorescence probe measurement of the intralysosomal pH in living cells and the perturbation of pH by various agents. *Proceedings of the National Academy of Sciences of the United States of America* **75**, 3327-3331 (1978).
114. Ohkuma, S., Moriyama, Y. & Takano, T. Identification and characterization of a proton pump on lysosomes by fluorescein-isothiocyanate-dextran fluorescence. *Proceedings of the National Academy of Sciences of the United States of America* **79**, 2758-2762 (1982).
115. Megason, S.G. & Fraser, S.E. Imaging in Systems Biology. *Cell* **130**, 784-795 (2007).
116. Pepperkok, R. & Ellenberg, J. High-throughput fluorescence microscopy for systems biology. *Nat Rev Mol Cell Biol* **7**, 690-696 (2006).
117. Rigler, R., Orrit, M. & BaschÃ©, T. *Single molecule spectroscopy : Nobel conference lectures*, (Springer, XBerlin, 2001).
118. Heiple, J. & Taylor, D. Intracellular pH in single motile cells. *J. Cell Biol.* **86**, 885-890 (1980).
119. Tycko, B. & Maxfield, F.R. Rapid acidification of endocytic vesicles containing Î±₂-macroglobulin. *Cell* **28**, 643-651 (1982).
120. Murphy, R., Jorgensen, E. & Cantor, C. Kinetics of histone endocytosis in Chinese hamster ovary cells. A flow cytofluorometric analysis. *J. Biol. Chem.* **257**, 1695-1701 (1982).
121. Wolfbeis, O.S., Fürlinger, E., Kroneis, H. & Marsoner, H. Fluorimetric analysis. *Fresenius' Journal of Analytical Chemistry* **314**, 119-124 (1983).
122. Giuliano, K.A. & Gillies, R.J. Determination of intracellular pH of BALB/c-3T3 cells using the fluorescence of pyranine. *Analytical Biochemistry* **167**, 362-371 (1987).
123. Caroline, C.O., Kyung-Dall, L., Eric, B. & Peter, J.H. Quantitative Measurement of Intraorganelle pH in the Endosomal-Lysosomal Pathway in Neurons by Using Ratiometric Imaging with Pyranine. *Proceedings of the National Academy of Sciences of the United States of America* **92**, 3156-3160 (1995).
124. McNeil, P., Tanasugarn, L., Meigs, J. & Taylor, D. Acidification of phagosomes is initiated before lysosomal enzyme activity is detected. *J. Cell Biol.* **97**, 692-702 (1983).
125. Cao, Y. et al. Relationship of proton release at the extracellular surface to deprotonation of the schiff base in the bacteriorhodopsin photocycle. *Biophysical journal* **68**, 1518-1530 (1995).
126. Paula, S., Volkov, A.G., Van Hoek, A.N., Haines, T.H. & Deamer, D.W. Permeation of protons, potassium ions, and small polar molecules through phospholipid bilayers as a function of membrane thickness. *Biophysical journal* **70**, 339-348 (1996).

127. Debbie, W., Roger, C.T. & Christof, J.S. The effects of intracellular pH changes on resting cytosolic calcium in voltage-clamped snail neurones. *The Journal of Physiology* **530**, 405-416 (2001).
128. He, X. & Rechnitz, G.A. Linear Response Function for Fluorescence-Based Fiber-Optic CO2 Sensors. *Analytical chemistry* **67**, 2264-2268 (2002).
129. Shingles, R. & Moroney, J.V. Measurement of Carbonic Anhydrase Activity Using a Sensitive Fluorometric Assay. *Analytical Biochemistry* **252**, 190-197 (1997).
130. Noji, H. et al. Purine, but not pyrimidine, nucleotides support rotation of F1-ATPase. *J. Biol. Chem.*, M102200200 (2001).
131. Dioumaev, A.K. et al. Existence of a Proton Transfer Chain in Bacteriorhodopsin: Participation of Glu-194 in the Release of Protons to the Extracellular Surfaceâ€ *Biochemistry* **37**, 2496-2506 (1998).
132. Montcourrier, P. et al. Characterization of very acidic phagosomes in breast cancer cells and their association with invasion. *J Cell Sci* **107**, 2381-2391 (1994).
133. Melikyan, G., White, J. & Cohen, F. GPI-anchored influenza hemagglutinin induces hemifusion to both red blood cell and planar bilayer membranes. *J. Cell Biol.* **131**, 679-691 (1995).
134. Miller, C.R., Bondurant, B., McLean, S.D., McGovern, K.A. & O'Brien, D.F. Liposomeâ^'Cell Interactions in Vitro: Effect of Liposome Surface Charge on the Binding and Endocytosis of Conventional and Sterically Stabilized Liposomesâ€ *Biochemistry* **37**, 12875-12883 (1998).
135. Kirpotin, D. et al. Sterically Stabilized Anti-HER2 Immunoliposomes: Design and Targeting to Human Breast Cancer Cells in Vitroâ€ *Biochemistry* **36**, 66-75 (1997).
136. Spragg, D.D. et al. Immunotargeting of liposomes to activated vascular endothelial cells: A strategy for site-selective delivery in the cardiovascularâ€‰system. *Proceedings of the National Academy of Sciences of the United States of America* **94**, 8795-8800 (1997).
137. Kutchai, H. Monitoring volume changes in red cell ghosts by means of a trapped fluorescent probe. *Journal of Biochemical and Biophysical Methods* **4**, 321-327 (1981).
138. Nomura, T., Escabi-Perez, J.R., Sunamoto, J. & Fendler, J.H. Aspects of artificial photosynthesis. Energy transfer in cationic surfactant vesicles. *Journal of the American Chemical Society* **102**, 1484-1488 (2002).
139. Clement, N.R. & Gould, J.M. Viscosity of the internal aqueous phase of unilamellar phospholipid vesicles. *Archives of Biochemistry and Biophysics* **202**, 650-652 (1980).
140. Lutty, G.A. The acute intravenous toxicity of biological stains, dyes, and other fluorescent substances. *Toxicology and Applied Pharmacology* **44**, 225-249 (1978).
141. Hillekamp, F.K., M.; Beavis, R. C.; Chait, B. T. Matrix assisted laser desorption/ionization mass spectrometry. *Analytical Chemistry* **63**, 1193-1203 (1991).
142. Chaurand, P.S., S. A.; Caprioli, R. M. Profiling and imaging proteins in tissue sections by MS. *Analytical Chemistry* **76**, 86A–93A (2004).
143. Karas, M.H., F. Laser desorption ionization of proteins with molecular masses exceeding 10,000 daltons. *Analytical Chemistry* **60**, 2299-2301 (1988).

144. Karas, M.K., R. Ion Formation in MALDI: The Cluster Ionization Mechanism. *Chemical reviews* **103**, 427-439 (2003).
145. Tanaka, K.W., H.; Ido, Y.; Akita, S.; Yoshida, Y.; Yoshida, T. Protein and Polymer Analyses up to m/z 100,000 by Laser Ionization Time-of-flight Mass Spectrometry. *Rapid Communications in Mass Spectrometry* **2**, 151-153 (1988).
146. Wells, J.M.M., S. A. (). "". Meth. Enzymol. : . Collision-induced dissociation (CID) of peptides and proteins. *Methods in enzymology* **402**, 148-85 (2005).
147. Sleno, L.V., D. A. . Ion activation methods for tandem mass spectrometry. *Journal of mass spectrometry* **39**, 1091-112 (2004).
148. Kosmidis, C.S., C.T.J.; Jia, W.; Ledingham, K.W.D.; Singhal, R.P. On the dynamics of the MALDI plume. *Quantum Electronics Conference, 1994., Proceedings of 5th European*, 87-87 (1994).
149. Dreisewerd, K. The desorption process in MALDI. *Chemical reviews* **103**, 395-426 (2003).
150. Breuker, K.K., R.; Zhang, J.; Stortelder, A.; Zenobi, R. Thermodynamic control of final ion distributions in MALDI: In-plume proton transfer reactions. *International Journal of Mass Spectrometry* **226**, 211–222 (2003).
151. Georgiou, S.H., F. Laser ablation of molecular substrates. *Chemical reviews* **103**, 317–644 (2003).
152. Knochenmuss, R.D., F.; Dale, M. J.; Zenobi, R. The Matrix Suppression Effect and Ionization Mechanisms in Matrix-assisted Laser Desorption/Ionization. *Rapid Communications in Mass Spectrometry* **10**, 871-877 (1996).
153. Kussmann, M.N., E.; Rahbek-Nielsen, H.; Haebel, S.; Rossel-Larsen, M.; Jakobsen, L.; Gobom, J.; Mirgorodskaya, E.; Kroll-Kristensen, A.; Palm, L.; Roepstorff, P. Matrix-assisted Laser Desorption/Ionization Mass
Spectrometry Sample Preparation Techniques
Designed for Various Peptide and Protein
Analytes. *Journal of Mass Spectrometry* **32**, 593-601 (1997).
154. Hanton, S.D.C.C., P.A.; Owens, K.G. Investigations of matrix-assisted laser desorption/ionization sample preparation by time-of-flight secondary ion mass spectrometry - Principles and Applications. *Journal of the American Society for Mass Spectrometry* **10**, 104-111 (1999).
155. Zenobi, R.K., R. Ion formation in MALDI mass spectrometry. *Mass Spectrometry Reviews* **17**, 337–366 (1998).
156. Schwartz, S.A.R., M. L.; Caprioli, R. M. Direct tissue analysis using
matrix-assisted laser desorption/ionization mass spectrometry:
Practical aspects of sample preparation. *Journal of Mass Spectrometry* **38**, 699–708 (2003).
157. Gomez, A. & Tang, K. Charge and fission of droplets in electrostatic sprays. *Physics of Fluids* **6**, 404-414 (1994).
158. Grimm, R.L.B., J.L. . Dynamics of Field-Induced Droplet Ionization: Time-Resolved Studies of Distortion, Jetting, and Progeny Formation from Charged and Neutral Methanol Droplets Exposed to Strong Electric Fields. *J. Phys. Chem. B* **109**, 8244-8250 (2005).
159. Grimm, R.L.B., J.L. . Field-Induced Droplet Ionization Mass Spectrometry. *J. Phys. Chem. B* **107**, 14161-14163 (2003).
160. Tabaei, S. Ultrasonically Levitated Droplet Ion Sources for Mass Spectrometry. *Masters Thesis, Department of Pure & Applied Biochemistry, Lund University* (2007).

161. Westphall, M.S.J., K.; Smith, L.M. Mass Spectrometry of Acoustically Levitated Droplets. *Anal. Chem.* **80**, 5847-5853 (2008).
162. Rapp, E.C., A.; Beinsen, A.; Plessmann, U.; Reichi, U.; Seidel-Morgenstern, A.; Urlaub, H.; Abel, B. . Atmospheric Pressure Free Liquid Infrared MALDI Mass Spectrometry: Toward a Combined ESI/MALDI-Liquid Chromatography Interface. *Anal. Chem.* **81**, 443-452 (2009).
163. Shiea, J.Y., C.H.; Huang, M.Z.; Cheng, S.C.; Ma, Y.L.; Tseng, W.L.; Chang, H.C.; Hung, W.C. . Detection of Native Protein Ions in Aqueous Solution Under Ambient Conditions by Electrospray Laser Desorption/Ionization Mass Spectrometry. *Anal. Chem.* **80** 4845-4852 (2008).
164. Rodbell, M. Metabolism of Isolated Fat Cells. I. Effects of hormones on glucose metabolism and lipolysis. *Journal of Biological Chemistry* **239**, 375-380 (1964).
165. Honnor, R.C.D., G. S.; Londos, C. cAMP-dependent Protein Kinase and Lipolysis in Rat Adipocytes. *Journal of Biological Chemistry* **260**, 15122-15129 (1985).
166. Rednikov, A.R., N. A simulation of streaming flows associated with acoustic levitators. *Physics of Fluids* **14**, 1502-1510 (2002).
167. Matsuura, N. et al. Screening System for the Maillard Reaction Inhibitor from Natural Product Extracts. *Journal of health science* **48**, 520-526 (2002).
168. Wrobel, K., Wrobel, K., Garay-Sevilla, M.E., Nava, L.E. & Malacara, J.M. Novel analytical approach to monitoring advanced glycosylation end products in human serum with on-line spectrophotometric and spectrofluorometric detection in a flow system. *Clin Chem* **43**, 1563-1569 (1997).
169. Kislinger, T., Humeny, A., Seeber, S., Becker, C.-M. & Pischetsrieder, M. Qualitative determination of early Maillard-products by MALDI-TOF mass spectrometry peptide mapping. *European Food Research and Technology* **215**, 65-71 (2002).
170. O'Harte, F.P.M. et al. Structure, antihyperglycemic activity and cellular actions of a novel diglycated human insulin. *Peptides* **21**, 1519-1526 (2000).
171. Gras, R.M., M.; Gasteiger, E.; Gay, S.; Binz, P.; Bienvenut, W.; Hoogland, C.; Sanchez, J.; Bairoch, A.; Hochstrasser, D. F.; Appel, R. D. Improving protein identification from peptide mass
fingerprinting through a parameterized multi-level scoring algorithm and an optimized peak detection. *Electrophoresis* **20**, 3535-3550 (1999).
172. Mantini, D.P., F.; Boccio, P.; Pieragostino, D.; Nicola, M.; Lugaresi, A.; Federici, G.; Sacchetta, P.; Di Ilio, C.; Urbani, A. Independent component analysis for the extraction of reliable protein signal profiles from MALDI-TOF mass spectra. *Structural bioinformatics* **24**, 63-70 (2008).
173. Mie, A.R., A.; Axelsson, B.O.; Jorntén-Karlsson, M.; Reimann, C.T. . Terbutaline Enantiomeric Separation and Quantification by Complexation and Field Asymmetric Ion Mobility Spectrometry-Tandem Mass Spectrometry. *Anal. Chem.* **80**, 4133-4140 (2008).
174. Mie, A.S., M.; Mathiasson, L.; Emnéus, J.; Reimann, C.T. . Analysis of Triazines and Associated Metabolites with Electrospray Ionization Field-Asymmetric Ion Mobility/Mass Spectrometry. *Anal. Sci* **24**, 973-978 (2008).